ISSN 2087-3840; e-ISSN 2774-9320

WOOD RESEARCH Journal

Journal of Indonesian Wood Research Society

Volume 12, Number 1, April 2021

Volume 12, Number 1, April 2021 ISSN 2087-3840; e-ISSN 2774-9320

WOOD RESEARCH Journal

Journal of Indonesian Wood Research Society

Chief Editor

Prof. Wahyu Dwianto

Editorial Board Members

Prof. Yusuf Sudo Hadi
Prof. Bambang Subiyanto
Prof. Wasrin Syafii
Prof. Anita Firmanti
Dr. Joko Sulistyo
Prof. Nobuaki Hattori
Prof. Jugo Ilic
Prof. Edi Suhaimi Bakar
Prof. Sri Nugroho Marsoem
Prof. Imam Wahyudi
Dr. Krisdianto
Dr. Ganis Lukmandaru
Dr. Tomy Listyanto
Dr. Ratih Damayanti
Fanny Hidayati, Ph.D.

Peer Reviewers

Indonesian Institute of Sciences
Prof. Subyakto
Prof. Myrtha Karina
Dr. Puspita Lisdiyanti

Bogor Agricultural University
Prof. Fauzi Febrianto
Prof. I Wayan Darmawan
Dr. Naresworo Nugroho

Gajah Mada University
Dr. Ragil Widyorini

Mulawarman University
Dr. Rudianto Amirta
Dr. Irawan W. Kusuma

Hasanuddin University
Prof. Musrizal Muin

Tanjungpura University
Prof. Yuliati Indrayani

Kyoto University
Prof. Junji Sugiyama
Prof. Toshiaki Umezawa
Prof. Takashi Watanabe

Dresden University
Dr. Christian Gottlöber

Oklahoma State University
Prof. Salim Hiziroglu

Montpelier University
Prof. Joseph P. Grill

Duzce University
Prof. Cihat Tasciouglu, Ph.D

Kangwon National University
Prof. Nam-Hun Kim

University of Melbourne
Prof. Barbara Ozarska

Paris Tech Cluny
Prof. Remy Marchal

Universiti Putra Malaysia
Prof. Edi Suhaimi Bakar

Journal Manager	Dr. Ratih Damayanti
IT Manager	Suhardi Mardiansyah, A.Md.
Section Editors & Initial Reviewers	Dr. Ratih Damayanti, Fanny Hidayati, Ph.D. Dian Anggraini Indrawan, S.Hut., M.M.
Copy & Layout Editor	Suhardi Mardiansyah, A.Md.
Proof Readers	Prof. Subyakto Dr. Krisdianto Dr. Tomy Listyanto
Treasurer	Dr. Firda Aulya Syamani, M.Si.

Spectroscopic and Non-destructive Analysis Methods for Investigation of Inorganic Pigments on Historical Wooden Objects in North of Iran

Faramarz Rostami-Charati, Gholamreza Rahmani, Roya Bahadori, and Farah Sadat Madani

Abstract

In this research, the characterization of very stable pigments from a cultural heritage building named by *Saghatalar* which is located in Mazandaran province, a suburb around of Fridonkenar city in the north of Iran near Caspian Sea (Cochakbishehmahaleh village) was investigated. For this investigation, the wood samples were given from *Saghatalar* for characterization and analysis. The result were showed no organic materials was find in the four colours (blue, red, yellow and green) as samples of this building were detected and taken. Fourier transform infrared spectroscopy (FT-IR), X-ray fluorescence spectroscopy (XRF), X-ray emission spectroscopy (XRD), Uv-vis spectroscopy, fluorescence spectroscopy, Raman spectroscopy and Mossbauer spectroscopy have been used for determination of kind of dyes in *Saghatalar* wood.

Keywords: Iran's Cultural Heritage, Saghatalar, Mazandaran province, X-ray, spectroscopy, Raman spectroscopy.

Introduction

There is no indication of the direct use of wood by the earliest hominids, although Neanderthals exhibited much complex behaviour such as funerary practices (Errico *et al.* 2012). Cultural uses of wood appear to be related to the activity of humans rather than hominids (Bamford 2010). Any wooden artefact that provides us information about human life and culture, and that is considered worthy of preservation for the future can be defined as wooden cultural heritage (WCH) (Rowell 1990). Vocational, technical artefacts, creative activities, and cannons of craftsmanship are embedded in WCH, reflecting past human culture, ideals, and symbols. Thus, the technological and sociological aspects of human activities can be understood from excavating WCH objects or remains. Wooden artifacts, wood painted panels and historic furniture represent a significant part of our cultural heritage. Their preservation over time is a challenging task as they can be damaged by several chemical–physical, mechanical and biological phenomena. The last ones are particularly relevant in causing damage, given the organic composition of wood. The microbiological activity of bacteria and fungi results in aesthetic alterations and depletion of mechanical characteristics, but insect infestation still represents a primary cause of loss of cultural heritage artifacts.

In the past, several chemical methods mainly based on the use of liquid preservatives or gaseous fumigants have been used for the conservation of wood under insect attack (Unger 2012). Such treatments present numerous negative drawbacks, including a high risk of damaging the objects (Wörle *et al*. 2012) and serious safety issues for operators due to chemical toxicity. Less dangerous alternatives have, therefore, been proposed and tested, including thermal treatment (using either low or high temperature) (Strang 1995), physical methods (microwaves, X-rays and gamma rays irradiation) (Andreuccetti *et al.* 1995; Augelli *et al.* 2007) and the use of controlled atmosphere (Unger *et al.* 2001). The colour in Cultural Heritage represents one of the latest international and interdisciplinary efforts in perfecting documentation of extant material cultural heritage. In the field of art conservation, the need to study colour and its variations became particularly evident in the second half of the 19th century when, following remarkable developments in the chemical industry, artists were provided with ready to use pigments/dyes (Bacci *et al.* 2006). Amongst scientific methods introduced to art conservation the measurement of the colour of any material or surface of artwork has been increasingly used from the 1930s (Barnes 1938; Johnston 1967; Bullock 1978).

A multi-technique analytical approach for the identification of pigments used to create wall paintings is crucial for a deeper knowledge of raw materials, manufacturing techniques and preservation methodology. Several works have been recently published on the characterization of pigments from cultural heritage artifacts using Fiber Optics Reflectance Spectroscopy (FORS) and Raman and X-Ray Fluorescence (XRF) portable equipment (Cheilakou *et al.* 2014; Aceto *et al.* 2014; Appolonia *et al.* 2009; Bracci *et al.* 2009 Syta *et al.* 2014: Madariaga *et al.* 2014), which are applied together in some cases. The imaging spectroscopy techniques can be effectively used for the identification of materials in artwork. The recent advances in the spectro-imaging field in addition to the demand for non-invasive techniques in the study of cultural heritage materials offer a favourable condition for the development of these methods. However, these techniques are usually not conclusive for identifying pigments; thus, confirmation of the composition through other experimental techniques is required. The inadequacies of FORS are observed when mixtures of pigments or organic binders are present (Cheilakou *et al.* 2014; Appolonia *et al.* 2009). XRF is elemental analytical technique that only yields information about key chemical elements. The employment of Raman equipment is only reliable when absolute stability is reached, and analysis using this technique takes a long time. In addition, the sensitivity and lateral resolution does not typically allow for the obtaining of information about all layers of the polychrome painting (Perez-Rodriguez *et al.* 2014). Some pigments also fail to produce an identifiable Raman spectrum, and others do not even produce a detectable signal (Duran *et al.* 2011). To overcome these difficulties, we have employed X-Ray Diffraction (XRD) in this work using a portable system, together with FORS and XRF. Only a few XRD portable systems are available at present (Beck *et al.* 2014; Mendoza-Cuevas *et al.* 2015; Nakai and Abe 2012; Pappalardo *et al.* 2008). XRD is the most consistent technique for the identification of crystalline materials, allowing for the identification of each component in a mixture.

The aim of the present work is to analysis several fragments of Roman wall paintings from an archaeological excavation of the Reales Alcazares Palace in Seville, dated between the first and second century AD. The chemical composition of pigments is responsible for the colour of the paintings (Edreira *et al.* 2001; 2003). The wood of these Iranian historical building with fantastic architecture are called *Saghatalar* which are specially located in the north of Iran (Mazandaran province) and firstly it was used as a local building as watchtower for agriculture forms. After one and half century, innovation, employing a professional manual activation and best architecture arts on that, their application were changed to religion and holy place in order to do the solemnize rite at MOHARRAM time. The used wood in this historical building is a local tree by name of *Zelkova carpinifolia* with high density and hardness characterization. For this question it is mentionable that the wood of this building is very hard and has a high density to be resistance in climate condition specially humidify and rainy whether of north of Iran. But it could a good layer for conservation and restoration of the wood. The painting on the wood has an invaluable message of the culture and the style of life of the people from the north of Iran. There is another *Saghatalar* that showed the life style and culture of the local people. This study attempts to establish an appropriate methodology for the complete characterization of the pigments by combining portable UV–Visible-FORS and XRF-XRD portable equipment. As far as we know, this is the first study to combine the use of UV–Visible-FORS and XRD portable equipment to analysis mural paintings.

Materials and Methods

The all reagents and solvents were purchased from Merck and used without further purification. Sampling in historical objects and buildings is one of the most sensitive parts in starting research work in the field of cultural heritage and sampling should be as little as possible and with the least damage on the object or monument. All works were carried out at room temperature in air.

Infra-red spectra were obtained on a Nicolet 510P FT-IR spectrometer. Scanning electron microscopies were performed on a Philips XL-300 instrument. UV-Vis spectrophotometric analysis was obtained on the Aventes UV4200 Avaspec spectrometer with Drift accessory. The morphology of wood sample was determined by the field emission scanning electron microscopy (Mira 3-XMU FESEM, Tescan Co, Brno, Czech Republic). The crystalline structure of wood sample was characterized by X-ray diffraction (XRD) analysis at room temperature using a Holland Philips Xpert X-ray powder diffractometer.

Preparing the Colour Samples

The acetone solvent was used for removing the sample colour with the appropriate technique. Therefore impregnating a small amount of cotton (2 g) by acetone and mechanically applied on the desired colour several times and the colour is separated from the wood as shown in the Fig. 1.

a) b)

Figure 1. a) Perspective of roof structure of *Saghatalar*, b) pigment wood samples.

The colour enters the cotton villi, in which the mineral pigments sample can be removed from the cotton by beating or re-dipping with solvent. In the step, the sample of mineral pigments can be removed from the cotton by beating or re-washing with immersion solvent. However, depending on the type of adhesive and substrate used, different solvents such as acetone (C_3H_6O), tetrahydrofuran (C_4H_8O), ethyl acetate ($C_4H_8O_2$) or paraloid can be used.

Results and Discussion

Pigments were first identified by means of XRF analysis according to the X-ray characteristic energies (keV) in each spectrum, corresponding to specific chemical elements. Attribution of different pigments is based on previous consideration from literature (Augelli *et al.* 2007). FT-Raman spectra provided more information on the pigments, while FTIR spectra gave more information on the organic content of painting.

FTIR of Pigments

According to previous studies, having a peak in the specified points in the FTIR spectrum in the Fig. 2 is related to artificial azure blue. Absorption bands in the 1020 cm^{-1} show the indicator peaks related to the azure colour. Other absorption bands in 1383 and 873 cm^{-1} are related to calcium carbonate ($CaCO_3$). The peaks with the numbers 603, 673 and 1113 cm^{-1} are related to the absorption index (gypsum or gypsum plaster). It should be noted that most of the dyes used in *Saghatalars* are associated with a mixture of oils and generally have organic esters carbonyl functional groups and appear in 1730 cm^{-1}. In this sample, because it was first washed with acetone and methanol in the preparation process and most of the esterified oily substances were removed, practically no carbonyl functional group is seen in the IR structure (Fig. 2). In the area above 3000 cm^{-1}, it shows the spectra of organic compounds in the pigment mixture as well as the wood texture introduced into the sample unintentionally during sampling (http://lisa.chem.ut.ee/IR_spectra/paint/pigments/lapis-lazuli). The next pigment tested in this structure is red pigment, which has slightly decreased in colour and has the IR spectrum as follows and in the IR spectrum, the index peaks represent the red colour (Ochre). In the FTIR spectrum, most indicators are related to the Ochre red, which also shows the peak of oils and associated adhesives in the carbonyl ester group at 1730 cm^{-1}. In this case, it has iron oxide compounds with the formula Fe_2O_3 with a high percentage and also a lower percentage of Pb_3O_4, which is attributed to the Ochre Red. The FTIR spectrum of green pigments in the range of 3000 and above has become a wide and indistinct peak, which has made detection a little difficult. The wide peak of the 3327 cm^{-1} region shows most of the hydroxy functional groups that entered the sample from the wood texture at the time of sampling (http://lisa.chem.ut.ee/IR_ spectra/paint/pigments/red-ochre-from-south-estonia, http://lisa.chem.ut.ee/IR_spectra/paint/pigments/italian-gold-ochre-light).

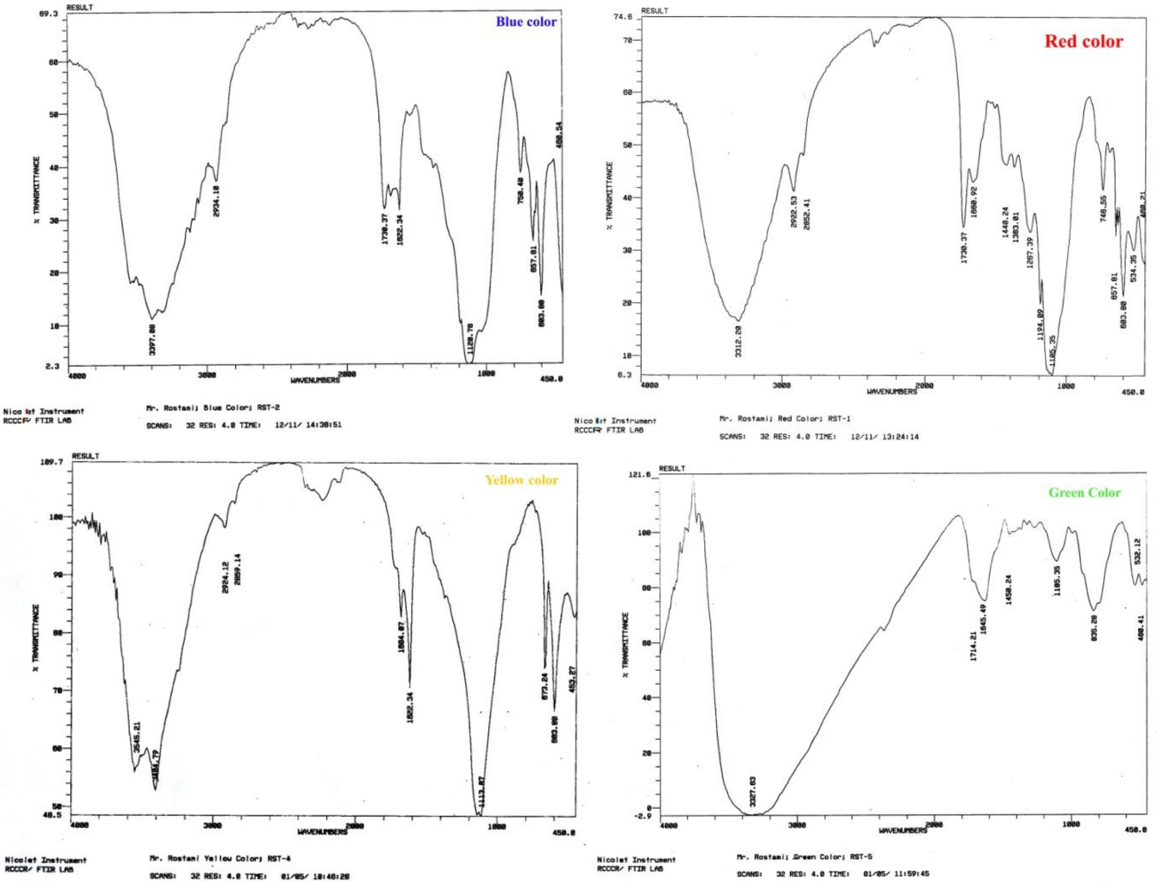

Figure 2. The IR spectrum of pigments.

SEM Images of Pigments

The morphological features of commercial pigments were investigated by scanning electron microscopy (Fig. 3). The SEM micrographs revealed that particles of each pigment are differently shaped and of unequal size (from tens to hundreds microns). The representative SEM micrograph of four colour of *Saghatalar* wood sample is given in Fig. 3.

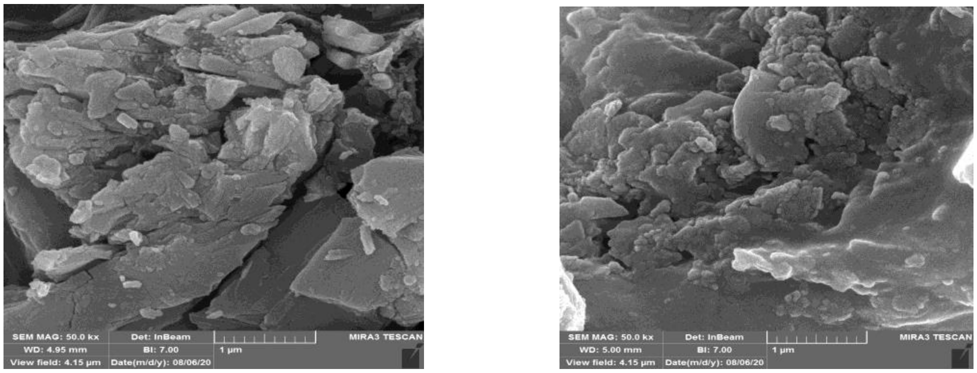

SEM image of blue color

SEM image of red color

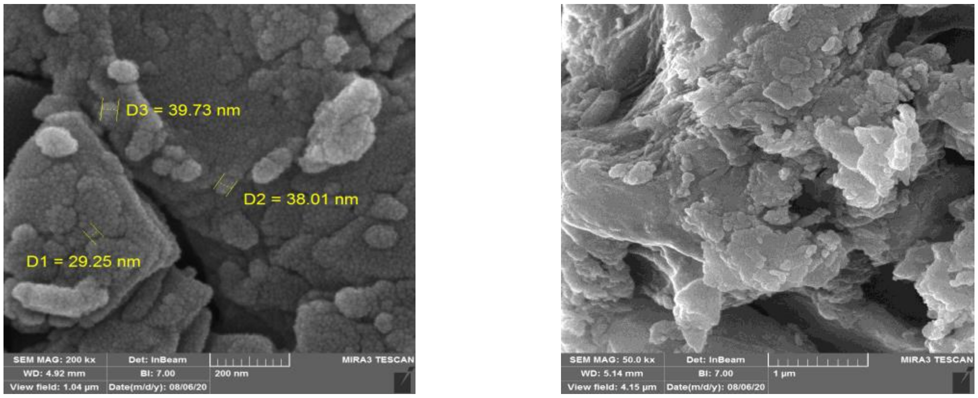

SEM image of yellow color

SEM image of green color

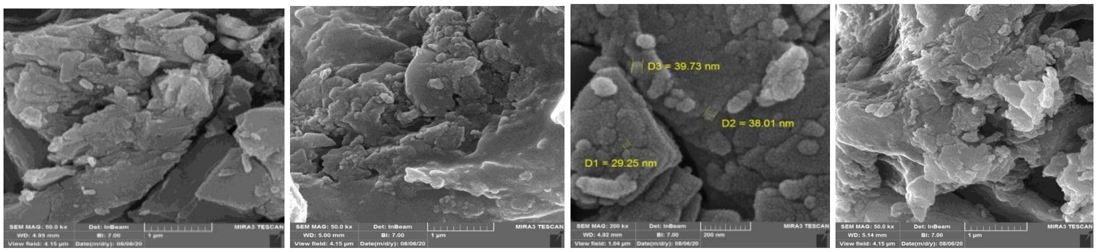

Blue

Red

Yellow

Green

Figure 3. SEM image of pigments.

EDX Analysis of Pigments

Elemental analysis of the wood samples was performed using EDX technique (Fig. 4). As shown in Fig. 4, Cr, Fe, O, C, Mg, Cu and Si show the elements in the wood sample.

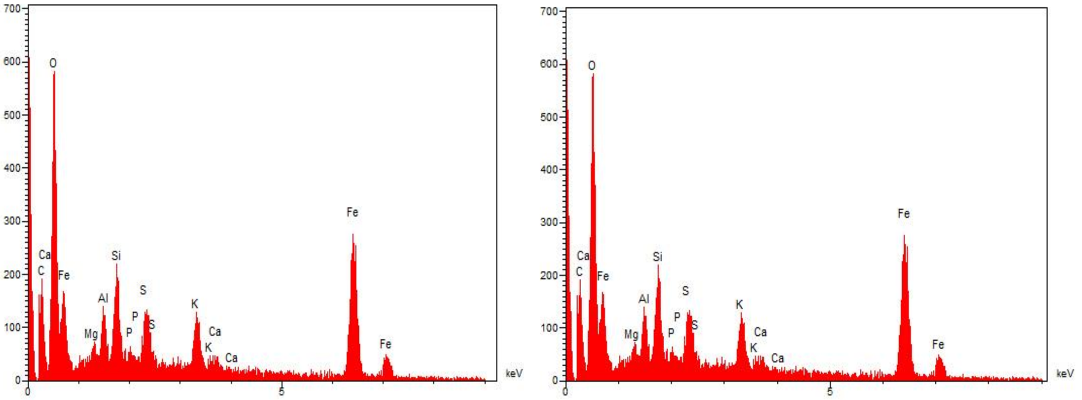

Blue Red

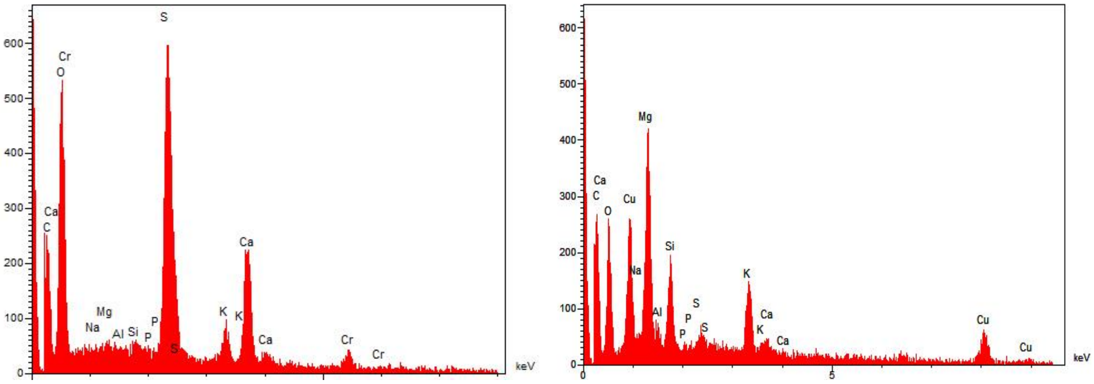

Yellow Green

Figure 4. EDX analysis of wood samples.

XRD Analysis of Pigments

Some of the most significant phases in these pigments in XRD show as a separate phase (Fig. 5). The sharp expression of calcium sulfate is gypsum. Therefore, because the amount of gypsum has a high percentage in the pigment mixture, which often shows sharper, peaks than the pigment. However, in the list of resulting peaks, in addition to gypsum, whose standard diagram is shown at the bottom of the diagram, the main peak has other peaks that are related to the structure of the main pigment and gypsum impurities.

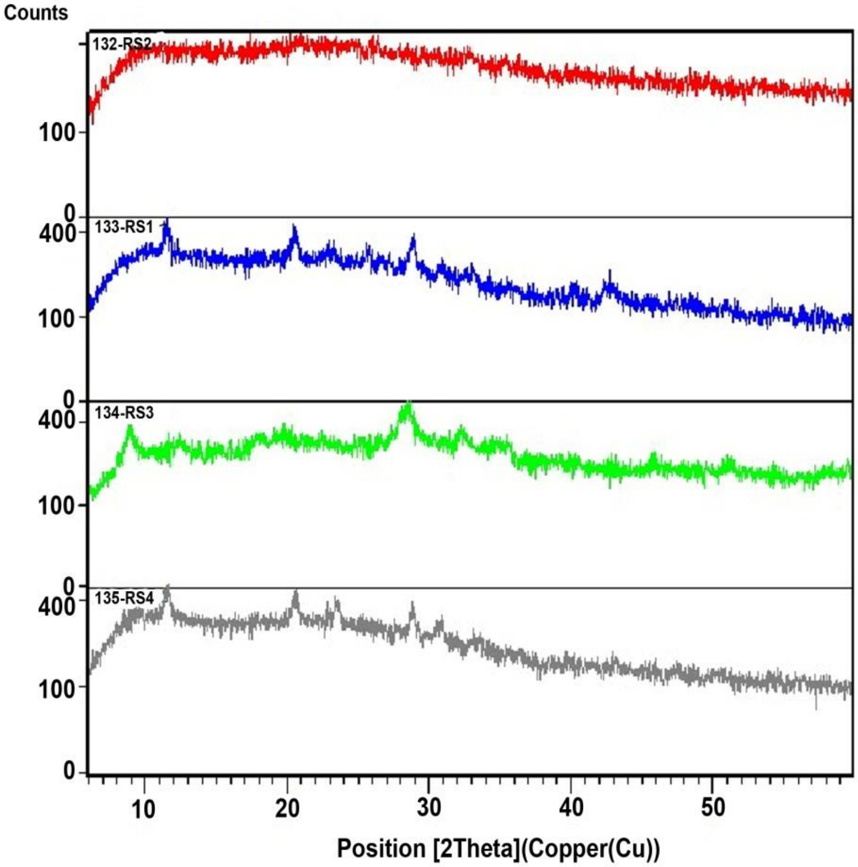

Figure 5. XRD analysis of four pigments in *Saghatalar* sample.

XRF Analysis of Pigments

In elemental analysis in XRF spectrum, the following items have been shown as the results of this spectroscopy and according to the formula of azure pigment Blue azurite $(NaCa)_8$ $[(SO_4SCl)$ - $(AlSiO_4)_6]$ and also in the composition of Blue amulet which are located on the wooden elements the following elements and compounds can be identified (Fig. 6). Indicative elements in this XRF spectrum are calcium 19.15%, potassium 17.99% and sulfur with 21.76% and silicon with 4.7% and it also has a lot of structural similarity compared to the standard azure blue spectrum (Standard IR-Spectra web address of Pigments) and is also decisive with other analysis results such as p-XRF and more chemical testing with acid and H_2S gas release. The chemical structure of this blue dye is confirmed by synthetic azure blue. According to the table below, the percentage of silicon, aluminum, and sulfur compounds in the blue pigment using elemental analysis can indicate the presence of artificial azure pigment as additional information.

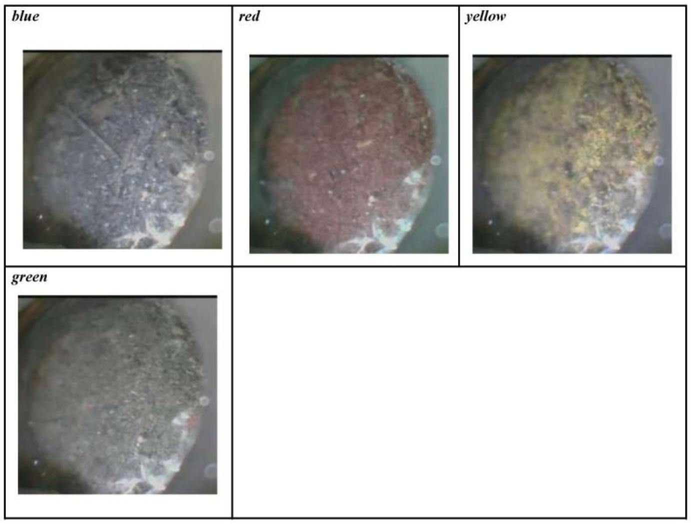

Figure 6. Four pigments in *Saghatalar* sample.

Table 1: XRF analysis of four pigments in *Saghatalar* sample

	Blue	Red	Yellow	Green	Tape
Sample	(%)				
Bal	30.83	43.23	40.482	48.903	66.045
Al	1.661	0.934	0.593	0.712	1.807
Si	4.759	3.534	4.124	2.296	9.964
P	0.43	0.506	0.541	0.275	1.189
S	21.76	8.421	20.683	4.501	12.750
Cl	0.73	0.478	0.859	0.590	2.303
K	17.99	7.541	2.463	4.490	-
Ca	19.18	2.478	24.588	2.873	1.983
Ti	0.21	0.102	-	0.031	0.048
Cr	0.02	0.070	1.063	-	-
Mn	-	-	0.164	0.034	-
Fe	1.24	30.817	1.450	0.35	0.25
Cu	0.76	0.655	0.669	18.322	1.175
Zn	0.02	0.293	0.029	-	-
Ba	0.02	0.024	0.323	0.016	0.039
As	0.09	0.532	0.433	16.387	0.009
Pb	0.19	0.301	1.477	0.179	0.007

The XRF analysis results of these four colours are summarized in the above Table 1. The Niton XL3t GOLDD + 950 portable XRF portable fluorescence spectroscopy device is of Thermo Scientific handheld portable type. It is noteworthy that the sample witnessed the book adhesive to which the colour powder of the four samples adhered and acted as a retaining substrate, and since it lacks mineral compounds, it is mainly organic compounds and has shown the least disturbance in the analysis.

Petrography Investigation of Four Colours

In this study, 4 samples of blue, red, yellow and green pigments obtained from *Saghatalars* have been analyzed and necessary. In this microscopic study (Fig. 7), the magnification of the device is 10x and observations have been made in polarized and cross-polarized light (XPL).

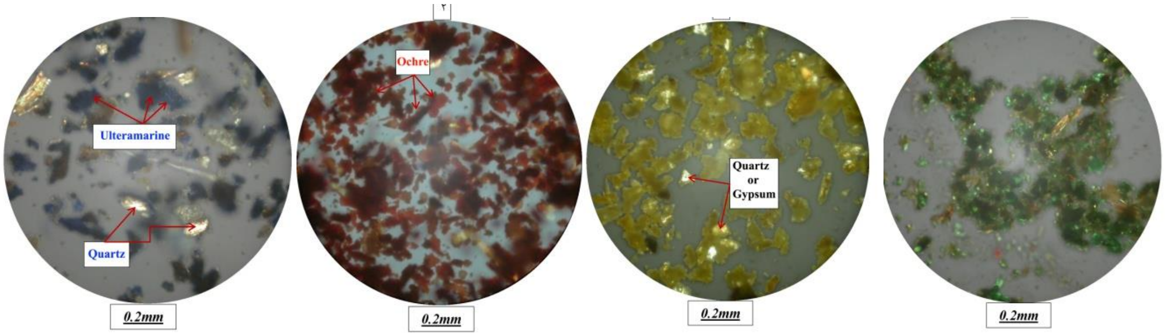

Figure 7. Petrography of four colours.

The details of the results obtained from petrography of blue pigment petrography are as follows. Or artificial azure has been identified by the chemical formula of the mineral lapis lazuli (Na_8 [$Al_6Si_6O_{24}$] Sn). Impurities are seen in the pigment. Finally, by microscopic examination of the red pigment, observing a high percentage of the target pigment, the "ochre" pigment is the most likely. The probable composition identified in the XRD analysis is gypsum, but its yellow colour can be attributed to a mixture of lead and iron oxide according to the XRF and FTIR results. Its microscopic studies also show cases such as quartz and gypsum.

Conclusions

In this study, In order to summarize the results obtained from the analyzes performed by FTIR, XRF, XRD and cross-sectional area and microscopic photographs in the petrographic laboratory on four categories of pigments extracted from the small woodpecker of Fereydunkenar neighborhood, the pigments used from. They were made of minerals and also organic materials such as gums and natural resins were used to fix the colour on the wood. Sometimes gypsum has been used to create a uniform composition with higher adhesion. The following results have been obtained by interpreting the spectra and data obtained from multiple analyzes obtained from FTIR, p-XRF, XRD and cross-sectional area and microscopic images of pigments extracted from the studied sciatica. Synthetic azure blue pigment with quartz crystals Blue azurite $(NaCa)_8$ [(SO_4SCl) - $(AlSiO_4)_6$], and ocher red pigment ocher $FexO_3$ and yellow composite Chromium yellow ($PbCrO_4$) is attributed to $PbSO_4$ lead sulfate as well as Scheele's Green ($CuHAsO_3$) green pigment. Of course, it should be noted that blue, red and yellow pigments and ester compounds of gum and resin can also be seen in the pigment. On the other hand, green and yellow colours in FTIR and XRD analyzes do not have good resolution and the peaks do not appear clearly and the most confirmation of its structure is based on XRF, which requires more professional analysis with EDX and SEM is that the necessary results can be obtained by comparing with references.

Acknowledgement

We gratefully acknowledge from Research institute of Cultural Heritage and Tourism, Tehran, Iran because of spiritual support.

References

Appolonia, L., Vaudan, D., Chatel,V., Aceto, M., Mirti, P. 2009. Combined use of FORS, XRF and Raman spectroscopy in the study of mural paintings in the Aosta Valley (Italy). Analytical and Bioanalytical Chemistry 395: 2005-2013.

Aceto, M., Agostino, Fenoglio, A. G., Idone, A., Gulmini, M., Picollo, M., Riccia-rdi, P., Delaney, J. K. 2014. Characterisation of colourants on illuminated manuscriptsby portable fibre optic UV-visible-NIR reflectance spectrophotometry. Analytical Methods journal 6: 1488-1510.

Andreuccetti, D., M. Bini, A. Ignesti, A. Gambetta, R. Olmi. 1995. Feasibility of microwave disinfestation of wood. In: Paper presented at the proceedings of 26th annual meeting IRG/WP, Helsingor, Denmark.

Augelli, F., B. Bisceglia, N. Diaferia, F. Foppiani, R. Tessari. 2007. L'impiego delle onde elettromagnetiche per la disinfestazione da organismi xilofagi (use of electromagnetic waves for disinfestation from xylophagous insects. La sperimentazione. Progetto Restauro 43: 2-11.

Bamford, M. 2010. Wood and Wooden Artefacts Among the Earliest Hominids in South and East Africa. Proc. Int. Wood Culture Symp., Shaanxi, China, 23-24.

Barnes, N. F. 1938. A spectrophotometric study of artists' pigments." Technical Studies in the Field of Fine Arts 7: 120-130.

Bullock, L. 1978. Reflectance Spectrophotometry for Measurement of Colour Change. National Gallery Technical Bulletin 2: 49-55.

Bracci, S., O. Caruso, M. Galeotti, R. Iannaccone, D. Magrini, D. Picchi, D. Pinna, S. Porcinai. 2009. Multidisciplinary approach for the study of an Egyptian coffin (late22nd/early 25th dynasty): combining imaging and spectroscopic techniques. Spectrochim. Acta A 145: 511-522.

Bacci, M., A. Casini, M. Picollo, B. Radicati, and L. Stefani. 2006. Integrated noninvasive technologies for the diagnosis and conservation of the cultural heritage. Journal of Neutron Research 14(1): 11-16.

Beck, L., H. Rousseliére, J. Castaing, A. Duran, M. Lebon, B. Moignard, F. Plassard. 2014. First use of portable system coupling X-ray diffraction and X-ray fluorescencefor in-situ analysis of prehistoric rock art. Talanta 129: 459-464.

Cheilakou, E., M. Troullinos, M. Koui. 2014. Identification of pigments on Byzantinewall paintings from Crete (14th century AD) using non-invasive Fiber OpticsDiffuse Reflectance Spectroscopy (FORS). Journal of Archaeological Science 41: 541-555.

Duran, A., M. L. Franquelo, M.A. Centeno, T. Espejo, J. L. 2011. Perez-Rodriguez, Forgerydetection on an Arabic illuminated manuscript by micro-Raman and X-rayfluorescence spectroscopy. Journal of Raman Spectroscopy 42: 48-55.

Errico, F., L. Backwell, P. Villa, I. Degano, J. Lucejko, M.K. Bamford, T.F.G., Highham, M.P. Colombini and P.B. Beaumont 2012; Early evidence of San material culture represented by organic artifacts from Border Cave, South Africa. Proc. Natl. Acad. Sci. USA 109: 13214-13219.

Edreira, M. C., M. J. Feliu, C. Fernández-Lorenzo, J. Martín. 2001. Roman wall paintingscharacterization from Cripta del Museo and Alcazaba in Mérida (Spain): chro-matic, energy dispersive X-ray fluorescence spectroscopic, X-ray diffractionand Fourier transform infrared spectroscopic analysis. Analytical Chimica Acta 434: 331-345.

Edreira, M. C., M. J. Feliu, C. Fernández-Lorenzo, J. Martín. 2003. Spectroscopic analysisof roman wall paintings from Casa del Mitreo in Emerita Augusta, Mérida, Spain. Talanta 59: 1117-1139.

Johnston, R.M. 1967. Spectrophotometry for the analysis and description of colour. Journal of Paint Technology 39 (509): 346-354.

Mendoza Cuevas, A., F. Bernardini, A. Gianoncelli, C. Tuniz. 2015. Energy dispersiveX-ray diffraction and fluorescence portable system for cultural heritage appli-cations." X-Ray Spectrom 44: 105-115.

Madariaga, J. M., M. Maguregui, S. F. O. de Vallejuelo, U. Knuutinen, K. Castro, I.Martinez-Arkarazo, A. Giakoumaki, A. Pitarch. 2014. In situ analysis with portableRaman and ED-XRF spectrometers for the diagnosis of the formation of efflo-rescence on walls and wall paintings of the Insula IX 3 (Pompeii, Italy)." J. RamanSpectrosc 45: 1059-1067.

Nakai, I., Y. Abe. 2012. Portable X-ray powder diffractometer for the analysis of artand archaeological materials. Applied Physics A: Materials Science and Processing 106: 279-293.

Pappalardo, L., G. Pappalardo, F. Amorini, M.G. Branciforti, F.P. Romano, J. deSanoit, F. Rizzo, E. Scafiri, A. Taormina, G. Gatto Rotondo. 2008. The complementaryuse of PIXE and XRD non-destructive portable systems for the quantitativeanalysis of painted surfaces. X-Ray Spectrom 37: 370-375.

Perez-Rodriguez, J. L., M. D. Robador, M.A. Centeno, B. Siguenza, A. Duran. 2014. Wallpaintings studied using Raman spectroscopy: a comparative study betweenvarious assays of cross-sections and external layers. Spectrochim Acta A 120: 602-609.

Rowell, R.M., R.J. (Eds.) Barbour. 1990. Archaeological Wood: Properties, Chemistry and Preservation. American Chemical Society, Washington, DC.

Syta, O., K. Rozum, M. Choinska, D. Zielinska, G.Z. Zukowska, A. Kijowska, B. Wagner. 2014. Analytical procedure for characterization of medieval wall-paintingsby X-ray fluorescence spectrometry, laser ablation inductively coupled plasmamass spectrometry and Raman spectroscopy. Spectrochim Acta A 101: 140-148.

Strang, T. J. K. 1995. The effect of thermal methods of pest control on museum collections. In: Proceedings of the 3rd international conference on biodeterioration of cultural property, Bangkok, Thailand.

Unger, A. 2012. Decontamination and ‘‘deconsolidation’’ of historical wood preservatives and wood consolidants in cultural heritage. Journal of Cultural Heritage 13: S196-S202.

Unger, A., A. Schniewind, W. Unger. 2001. Conservation of wood artifacts: a handbook. Springer, Berlin UNI 10829 (1999) Works of art of historical importance Ambient conditions or the conservation measurement and analysis.

Wörle, M, V. Hubert, E. Hildbrand, K. Hunger, E. Lehmann. 2012. Evaluation of decontamination methods of pesticide contaminated wooden objects in museum collections: efficiency of the treatments and influence on the wooden structure. Journal Cultural Heritage 13(3): S209-S215.

http://lisa.chem.ut.ee/IR_spectra/paint/pigments/lapis-lazuli

Faramarz Rostami-Charati*, Gholamreza Rahmani, Roya Bahadori, and Farah Sadat Madani
Research Center for Conservation of Culture Relics (RCCCR)
Research Institute of Culture Heritage and Tourism
Tehran, Iran
*Corresponding author: f_rostami_ch@yahoo.com, f.rostami@richt.ir

Extractive Content and Colour Properties of 11-Year-Old Superior Teak Wood

Ganis Lukmandaru, Alfian Nur Falaah, Tomy Listyanto, and Dian Rodiana

Abstract

As a fancy wood, teak is valued for beautiful grain and color. However, there is a lack of understanding about the properties of fast-growing teak trees harvested in young stage. In addition, wood variation in vertical direction is less investigated. Therefore, the objective of this research was to assess superior teak woods (11 years, 5 trees) grown in Pemalang FMU in vertical and radial positions for its extractive contents and colour. Extractions were conducted using a sequence of toluene, ethanol, and hot water. The color evaluation was performed using CIEL*a*b*'s chromaticity system. The contents of toluene-extract, ethanol extract, hot-water extract, and total extractive ranged between 1.16~5.00%; 0.29~1.04%, and 0.98~2.35%, and 4.03~7.31%, respectively. For color properties, the brightness (L*), redness (a*), and yellowness (b*) indices ranged from 49.50~57.42, 6.08~10.81, and 20.47~25.74, respectively. Toluene- and total extractive contents were greater in heartwood than in sapwood, while the reverse occurred for the hot-water extractive content. Toluene- and total extractive contents were higher in outer heartwood than in inner heartwood. With regard to colour properties, L* and a* values were significantly differed between sapwood and heartwood. Vertical stem analysis of samples obtained at bottom, center, and top showed the toluene extractive content, total extractive content, and a* levels of center part of the tree were found to be lower than other parts. The L* were negatively correlated with extractive contents, with the highest correlation degree (-0.83**) being observed in the total extractive content in the heartwood. This comparatively high level of correlation might be useful to predict its extractive amount as well as its natural durability. It is also noticed that superior teak wood was less darker and extractive contents than the heartwood control of a 72-year-old tree.

Keywords : juvenile wood, fast-growing, axial variation, wood chemistry, Jati Plus Perhutani.

Introduction

Teak (*Tectona grandis* L.f) is a crucial wood resource in Indonesia. The value of teak wood depends on its high natural durability, weather resistance, and beautiful color. Therefore, teak is utilized for various products and outdoor purposes. The qualities of teak wood are undoubtedly derived from extractives in the heartwood (Yamamoto *et al.* 1998; Lukmandaru and Takahashi 2008; 2009). Many studies have investigated that quinones are responsible for bioactivity against termites and fungi (Haupt *et al.* 2003; Thulasidas and Bhat 2007; Niamké *et al.* 2012; Lukmandaru 2013; Ismayati *et al.* 2016). Meanwhile, the relationship between color properties and natural durability has been addressed by several researchers (Bhat *et al.* 2005; Kokutse *et al*. 2006; Lukmandaru and Takahashi 2008).

The superior teak wood (Jati Plus Perhutani) from vegetative propagation has been utilized for various products. The trees were characterized by their faster-growing nature, unlike conventional trees. So far, superior teak wood has been harvested early. The teak wood from young trees is associated with a paler color and lower natural durability (Bhat and Florence 2003; Lukmandaru and Takahashi 2008). Unfortunately, there is little information about the color and natural durability of superior teak or fast-growing teak wood. Consumers necessarily have the basic knowledge to utilize these woods and produce the best advantages. Previously, the chemical components of superior teakwood (15 years) have been investigated (Lukmandaru *et al.* 2016). Furthermore, the relationship of the extractive content and color porperties of teak wood from young trees has been addressed but no clear pattern was found (Lukmandaru and Sayudha 2019; Zulkahfi *et al*. 2020). This study aimed to determine the extractive contents and color properties of superior teakwood. A factorial design was used to investigate the effects and interaction of vertical and radial positions. This study also discussed the correlation between the extractives' contents and the woods' colors.

Materials and Methods

The experiment was conducted in an 11-year-old teak stand (diameter breast height = 19.5~27.8 cm, heartwood proportion = 76.7~85.7%, growth rate = 1.77~2.52 cm/year) located in compartment 49, KRPH Klapanunggal, BKPH Banjar Sari, Pemalang Forest Management Unit, Central Java Province. The trees were selected to represent the young stage and currently were available in the market. All trees had been girdled for 13 months and five free-defect trees were felled at December 15, 2016. A 5-cm-thick disc was removed at three different vertical positions from the trees (Fig. 1). Each disc was divided into three parts: sapwood (SW), outer heartwood (OH), and inner heartwood (IH). Each part was converted into wood meal (40~60 mesh size) to determine the extractives content and color properties. The specimens from two cardinal radii (north-south) were then combined to form a single sample. Sample meals were also prepared from the heartwood of a 72-year-old tree (bottom part) located Randublatung FMU, Central

Java Province, for comparative purposes (control). This mature tree was expected to give sharp differences from the young trees.

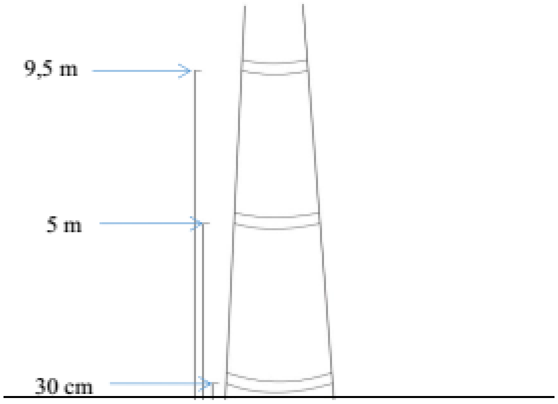

Figure 1. Diagrammatic illustration of discs removed from the vertical position of the tree.

Determination of Extractive Contents

Three grams of dried wood powder was successively extracted with toluene, ethanol, and hot water. The extractions were conducted using a 6-h sequence of toluene and ethanol using a Soxhlet apparatus. Hot-water extractives content was determined following the ASTM D-1110-1981 standard method. The solvents were concentrated in a rotary film evaporator, dried, and weighed to determine the toluene, ethanol, and hot-water extractive contents based on the oven-dry wood meal (m/m). The total of extractive contents was calculated by determining the sum of all extractive contents.

Color Measurement

The wood color was measured in the air-dried wood powder using an NF333 spectrocolorimeter (Nippon Denshoku Ind. Co Ltd.) with an opening diameter of 6.0 mm. Moreover, this measurement employed the CIE standard illuminant D65 and a tungsten halogen light source. The percentage of reflectance data was collected at 10-nm intervals over the visible spectrum (400~700 nm). Three measurements were made for each part. The value L* described psychometric lightness (0=black to 100=white). The value a* described the redness from the axis red (+) to green (–). Meanwhile, the value b* describes the yellowness from the Y axis yellow (+) to blue (–).

Statistical Analysis

The variation in the extractive contents and color properties was analyzed by two-way analysis of variance (ANOVA) followed by Duncan's multiple range test (p = 0.05). Meanwhile, the relationship between the independent variables was investigated using Pearson's correlation analysis. The data were analyzed by using SPSS-Win 16.0.

Results and Discussion

Extractive Contents

Extractive contents were obtained by successive extraction from apolar to polar solvents. Then, total extractive content was calculated. The values of toluene extractive, ethanol extractive, and hot-water extractive contents respectively ranged from 1.16~5.00%, 0.29~1.04%, and 0.98~2.35% (Table 1). It is found that toluene extractive content showed wider range compared to others. These values were lower than the corresponding values of control heartwood, particularly the values of toluene- and ethanol extractive contents. The corresponding values of toluene extractive content (TEC) of this study were within the range, unlike the values of previous studies. Meanwhile, the values of ethanol extractive content (EEC) were lower than those of 8~ and 31~year-old teak wood in community forest and 51-year-old teak wood from Perhutani plantation stand (Lukmandaru and Takahashi 2008). In addition, the values of hot-water extractive content (HWC) were within the range, unlike the values of teak from Perhutani (class age III~V) as reported by Lukmandaru (2010; 2016).

Total extractive content (TOC) of superior teak heartwood was considerably lower (4.03~7.31%) than that of the control mature heartwood (13.43%). These values were also lower than those of other mature teak heartwoods from Perhutani by 7.15-9.17% (Lukmandaru and Takahashi 2008) and 10.57~12.62% (Lukmandaru 2016). Regardless of the different sites, these findings correspond to the age-related trend generally observed by wood chemists.

The ANOVA of extractive contents showed no significant vertical and radial position interactions (Table 2). The radial direction denoted that heartwood and sapwood had statistically distinctive TEC, HWC, and TOC. Furthermore, TEC and TOC levels in the IH differed significantly from those in the OH (Fig. 2 and 3). The significant difference between OH and IH was also observed for mature teakwood but not for juvenile teakwood in an earlier report (Lukmandaru and Takahashi 2008). It indicates that synthesis and accumulation of extractives during heartwood formation are more intense in the outer heartwood region or more mature in the superior teak.

The ANOVA revealed that the vertical direction had significant differences. The TEC and TOC levels in the bottom and top parts were higher than those in the center part. The high content of TEC and TOC in the bottom part was probably caused by intense polymerization reactions during the aging process of the tree. Meanwhile, the high content in the top part was caused by the vicinity to the crown part as the photosynthesis site. The significant differences in vertical direction were also found in eucalypt hybrid urograndis from Brazil (Gominho *et al.* 2001). Yunanta *et al.* (2014) measured an increase in an ethanol-toluene extract with tree height of shorea species.

The EEC and HWC level variations in different vertical directions were insignificant. This finding suggested that high molecular weight phenolics and sugars remained steady with height. The patterns of HWC levels were similar to those of Siberian larch wood, which had no systematic differences in vertical position (Neverova *et al.* 2013). HWC tended to increase from the bottom to the top part in *Robinia pseudoacacia* (Adamopoulos *et al.* 2005). This finding differs from the present investigation's results.

Table 1. Extractive contents and color properties of superior teak wood (11 years, mean of 5 trees) as compared with a mature control. The same letters on the same column are not statistically different at $P < 0.05$ by Duncan's test.

		Extractive content (%)				Colour properties		
Vertical	Radial	TEC	EEC	HWC	TOC	L*	a*	b*
Bottom	Sapwood	1.74	0.29	2.53	4.57	60.87	6.94	20.47
	Outer heartwood	4.95	0.45	1.27	6.67	51.07	10.07	23.66
	Inner heartwood	4.02	0.36	1.14	5.52	52.64	10.81	23.18
	Average	3.57b	0.37	1.65	5.59cd	54.86	9.27g	22.44
Center	Sapwood	1.43	0.39	1.91	3.73	64.45	6.08	20.61
	Outer heartwood	4.03	0.39	0.98	5.73	51.97	9.94	24.34
	Inner heartwood	2.18	0.84	1.00	4.03	57.42	9.87	23.96
	Average	2.55a	0.54	1.30	4.50c	57.95	8.63f	22.97
Top	Sapwood	1.16	0.74	1.89	3.78	64.50	6.41	25.74
	Outer heartwood	5.00	1.04	1.18	7.31	49.50	10.48	24.86
	Inner heartwood	3.35	0.93	1.21	6.18	50.80	10.55	24.03
	Average	3.34b	0.90	1.43	5.76d	54.93	9.14 g	24.87
Control	Heartwood (72 years)	8.20	2.64	2.59	13.43	41.57	10.63	24.27

Remarks: TEC = toluene extractive content, EEC = ethanol extractive content, HWC = Hot-water extractive content, TOC = total extractive content.

Table 2. Vertical and radial direction analysis of variance in extractive contents and color properties of superior teak wood.

	df	Mean square						
Source of variation		TEC	EEC	HWC	TOC	L*	a*	b*
Vertical position (A)	2	4.36*	1.02	0.47	6.34*	45.17	1.69*	24.59
Radial position (B)	2	38.39*	0.29	4.83**	22.34*	622.24*	72.45*	15.65
A x B	4	1.52	0.05	0.18	1.52	24.17	0.36	11.52
Error	36	0.77	0.35	0.56	1.74	16.88	0.40	13.16

Remarks: TEC = toluene extractive content, EEC = ethanol extractive content, HWC = Hot-water extractive content, TOC = total extractive content. ** Significant at the 1% level; * significant at the 5% level

Toxic quinones were mostly detected in apolar fraction, while the predominantly sugar (mono- and disaccharides) and sugar derivatives were identified in the methanol extracts (Windeisen *et al*. 2003; Lukmandaru and Takahashi 2009). The low amounts of TEC and TOC probably cause lower natural durability in superior teakwood than in conventional mature teaks. The sapwood part in radial position or the center part in vertical position was susceptible. Many studies have discovered the relationships between extractive contents and resistance against termite or fungi (Haupt *et al.* 2003; Lukmandaru and Takahashi 2008; 2009; Lukmandaru 2011). Niamké *et al.* (2011) measured high concentrations of starch and low molecular weight sugars in the teak sapwood. The high levels of HWC in the sapwood might reduce the natural durability against fungi. This study found that the sapwood proportion in the superior teak samples was 20% to 40%.

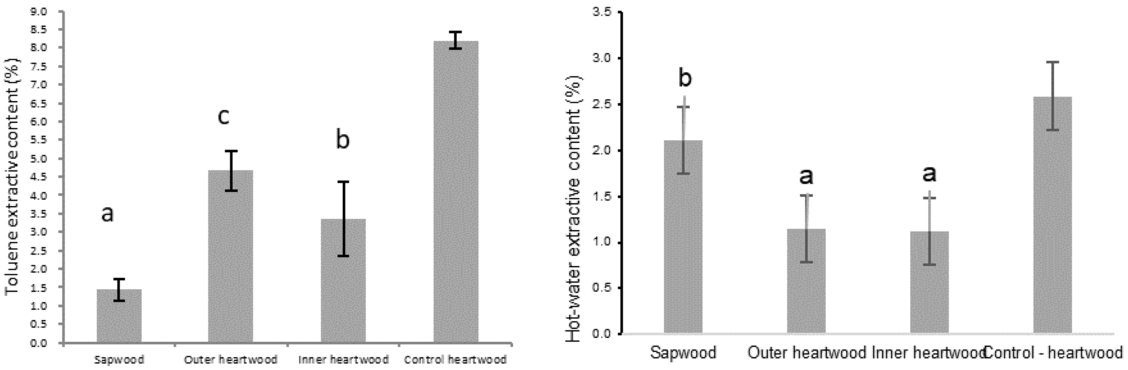

Figure 2. Extractive content obtained by successive extraction properties of superior teakwood (11 years) by radial position. Mean of 5 trees, with the standard deviation error bar. The same letters on the same graphic are not statistically different at $P < 0.05$ by Duncan's test.

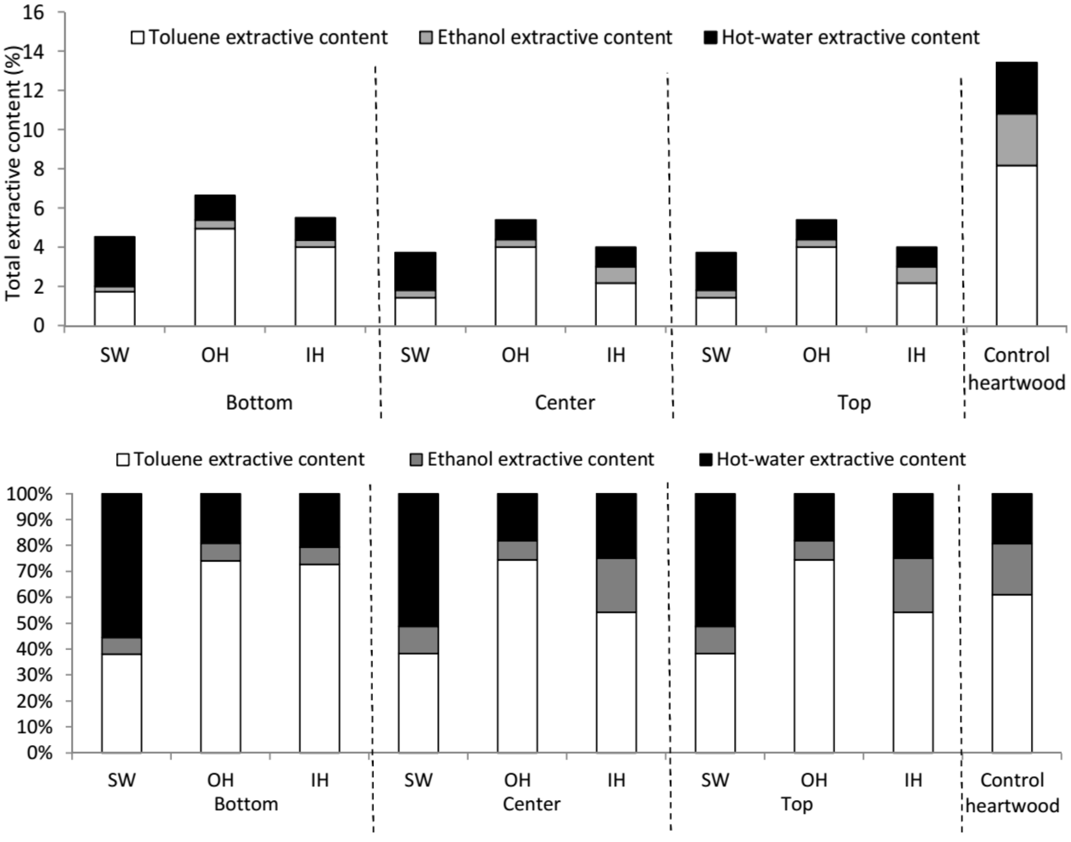

Figure 3. Total extractive content obtained by successive extraction of superior teakwood (11 years) based on oven-dry wood meal (upper) and extractive weight (lower). Remark : SW = sapwood; OH = outer heartwood, IH = inner heartwood.

Based on extractive weight, a clear distinction between sapwood and heartwood was found in TEC and HWC levels. The TEC level of the sapwood did not exceed 40%, and the HWC level of the heartwood did not exceed 30% (Fig. 3). The similarity between superior teak heartwood and mature heartwood control was the composition of extractive content of IH in the center and top parts. This finding showed the EEC levels were close to 20%, while the TEC levels did not exceed 70%. IH in the bottom part was characterized by a high amount of TEC and a low amount of EEC. It is assumed that sapwood has low natural durability due to the low content of TEC and EEC. IH part did not exhibit a similar level of natural durability to OH in other studies (Kokutse *et al.* 2006; Bhat *et al.* 2005). Although the IH of superior teakwood has the similar extractive content composition to that of heartwood control samples, the mature and juvenile woods have different compositions and content of toxic components (Lukmandaru and Takahashi 2009).

Color Properties

The L*a*b* values of superior teakwood samples and heartwood control had no striking differences, except the L* parameter (Table 1). The control sample's heartwood region had a significantly darker color (L* = 41.57) than the superior teakwood's (L* = 49.50~57.42). These values agreed with the general assumption that the heartwood of younger trees was paler, regardless of their different sites (Lukmandaru 2009a; Gierlinger *et al.* 2004). Moreover, the obtained values were nearly similar to the values of mature teak wood trees grown in Perhutani (Lukmandaru 2016).

The ANOVA of color properties showed no significant vertical and radial position interactions (Table 2). However, the L* and a* values of sapwood and heartwood differed significantly (Fig. 4). The ANOVA also revealed no significant difference in heartwood (OH and IH). Lukmandaru and Takahashi (2008) reported a significant difference in L* and a* between IH and OH of 51-year-old teak trees; this finding differs from the present investigation's findings. Studies on color properties of teak have noted similar patterns (Kokutse *et al.* 2006; Moya and Berrocal 2010). These patterns were probably related to the similar composition of coloring matters of the superior teakwood although TEC and TOC levels of OH and IH were statistically different. Vertical stem analysis discovered that the center part had statistically lower a* values than others, but in a small magnitude (Table 1).

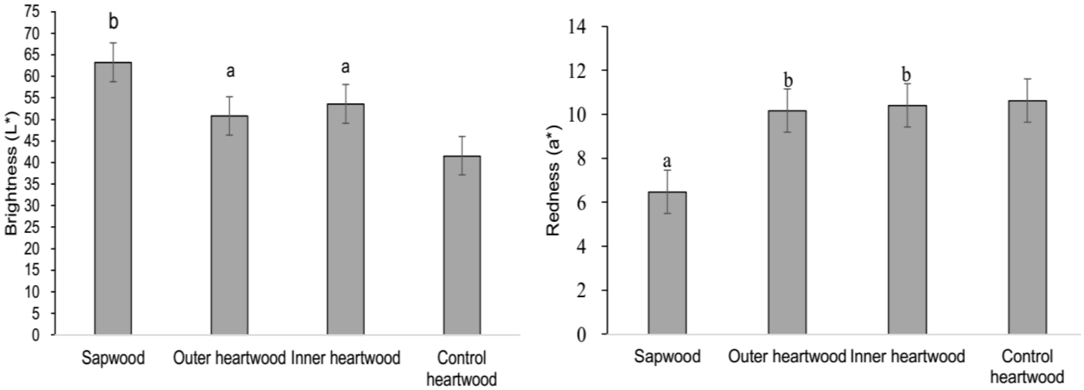

Figure 4. Color properties of superior teakwood (11 years) by radial position. Mean of 5 trees , with the standard deviation error bar. The same letters on the same graphic are not statistically different at $P < 0.05$ by Duncan's test.

Table 3. Pearson's correlation coefficients between extractive contents and color properties of superior teakwood (11 years)

	TEC	EEC	HWC	TOC
Sapwood				
Brightness (L*)	-0.26	0.05	-0.66**	-0.67**
Redness (a*)	0.19	-0.15	0.37	0.36
Yellowness (b*)	-0.02	0.23	-0.01	0.05
Heartwood				
Brightness (L*)	-0.63**	-0.55**	-0.24	-0.83**
Redness (a*)	0.43*	0.17	0.41*	0.51**
Yellowness (b*)	0.09	-0.11	-0.24	-0.02

Remark: TEC = toluene extractive content, EEC = ethanol extractive content, HWC = hot-water extractive content, TOC = total extractive content. ** Significant at the 1% level; * significant at the 5% level.

Wood color, together with beautiful grain, is an important quality parameter for teak. The inhomogeneity in vertical position (redness) and brighter heartwood in superior teak wood were certainly undesirable for several products (Table 1). Therefore, further research should modify superior teak wood to enhance its color properties. Heat treatment is used to improve the color properties and obtain a decorative specific dark color. So far, teak wood of young trees has been subjected to a heat treatment (Garcia *et al.* 2014).

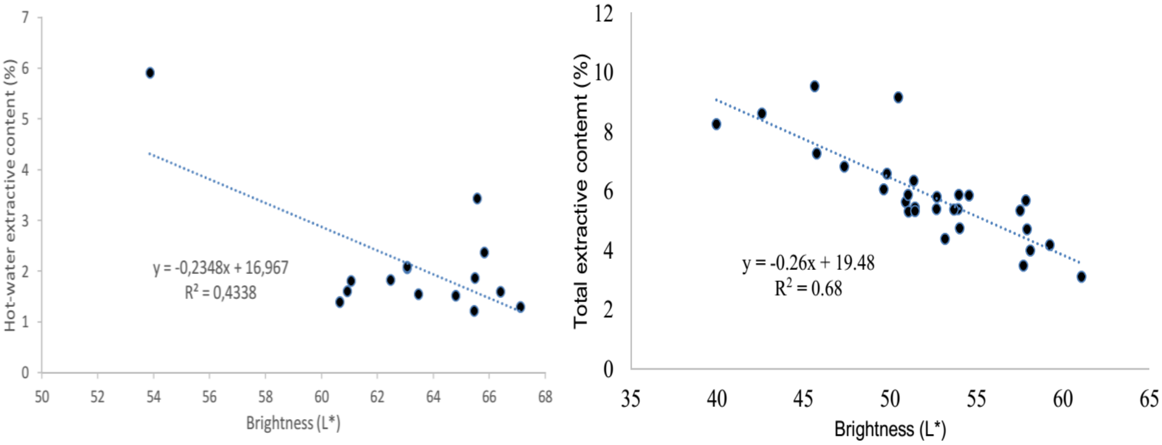

Figure 5. Scatterplots between hot-water extractive content and brightness (left) and between total extractive content and brightness (right) of superior teak wood (11 years).

Relationship between Extractive Contents and Color Properties

The correlation coefficient of sapwood and heartwood was considered as separated samples of color parameters and extractive contents. This correlation is summarized in Table 3. Table 3 confirms moderate negative correlation between the L* and HWC (*r* = -0.66**) and between the L* and TOC (*r* = -0.67**) in sapwood region. These slightly different values indicated that hot-water solubles mostly affected sapwood colors. This condition means that the sapwood contains more hot water soluble when it is darker (Fig. 5).

The measurement of L* and TOC values gained the highest negative correlation of *r* = -0.83** in the heartwood region (Table 3). This strong correlation degree was a combination of apolar and polar fraction, as seen in the moderate negative correlation between L* and TEC (*r* = -0.63**) or EEC (*r* = -0.55**). These findings denote that the TEC and EEC contribute equally, and wood is darker when it contains more toluene and ethanol soluble extracts. The correlation analysis also revealed a moderate positive correlation between a* and TOC values, a* and TEC values, as well as a* and HWC values in the heartwood part. There was no significant relationship between the b* and extractive content parameters. This finding signifies that the parameter a* increases when TEC, HWC, and TOC values increase. Various TEC, HWC, and TOC levels caused various a* values in the vertical position (Table 1). The relationship between extractive contents and color properties (L* and a*) was also found in normal and black-streaked heartwood teak (Lukmandaru *et al.* 2009b; Lukmandaru 2011).

This study discovered significant correlations indicating that phenolics or coloring matters affected brightness and redness in apolar and polar fractions. A previous work by Lukmandaru (2016) found moderate correlations between L* and ethanol-benzene extracts (*r* = -0.60*) as well as between a* and ethanol-benzene extracts (*r* = 0.39*) of mature teak grown in Perhutani. These different correlation degrees occurred in juvenile and mature trees, particularly in their composition of coloring matters.

The L* was strongly correlated with the TOC (*r* = -0.83), and thus, it was suitable for predicting the extractive amount (Fig. 5). The *n*-hexane and methanol extraction have detected several quinones (Lukmandaru 2013). Unfortunately, the contribution of quinones to wood color in teak has been less investigated. In addition, HWC was related to L* in sapwood and a* in the heartwood. The water-soluble coloring matters also remain unknown. The considerable differences of TEC and TOC levels between superior teak wood samples and mature heartwood control (Table 1) have corroborated these findings that teak wood color is associated with extractives' amounts. Many studies have found a positive correlation between the L* index and mass loss against termites (Lukmandaru and Takahashi 2008; Lukmandaru 2011) or against fungi (Kokutse *et al*. 2006) in teakwood. Therefore, further research necessarily investigates the use of fine teakwood and tests its natural durability.

Compared to the resuts of our parallel work (Zulkahfi *et al.* 2020) on superior teakwood (11 years) from Ngawi stand, several differences were found. The values of TEC and HWC in were higher but lower in ECC than those of Ngawi samples. Furthermore, the TOC values in top part in this experiment were higher. For color properties, with exception in top part, the heartwood of these Pemalang samples were darker than those of Ngawi woods. The differences pattern in longitudinal and radial variations on both extractive contents and color properties suggests a considerable geographical effect. With regard to relationship between extractive content and color properties, this finding confirm the significant correlation between L* and HWC in sapwood tissue of Ngawi sites. However, the similar pattern was not measured in the heartwood region, particularly in L* characteristic. In an earlier study (Lukmandaru and Sayudha 2019) for juvenile teakwood (5 and 7 years), HWC was moderately correlated with a* and b* levels (negatively) in heartwood part or with L* (negatively and a* (positively) in sapwood part. Therefore, it is assumed that color affecting phenolics in teakwood are varied in some extents even in young ages.

Acknowledgement

The authors are grateful to Perum Perhutani for its financial support of the research and Adminitrator of Ciamis FMU for providing the wood samples.

Conclusions

The investigation of all wood parameters (bottom, center, and top) showed that sapwood and heartwood had significantly different values in toluene extractive content, total extractive content, L*, and a* values. Moreover, the outer heartwood and inner heartwood had significantly different toluene extractive content and total extractive content. The toluene extractive content, total extractive content, and a* levels of the trees' center part were significantly lower than those of the bottom and top parts. This study also demonstrated that superior teak wood exhibited significantly fewer extractive contents than the mature control. Furthermore, superior teak samples showed a considerably brighter appearance than the mature control. The L* was strongly correlated with total extractive content levels in the heartwood region, and L* was moderately correlated with hot-water extractive content in the sapwood region. The less extractive content and brighter color in the heartwood were probably related to its natural durability, which was an essential characteristic of heartwood's utilization.

References

Adamopoulos, S.; E. Voulgaridis; C. Passialis. 2005. Variation of Certain Chemical Properties within the Stemwood of Black Locust (*Robinia pseudoacacia* L.). Holz als Roh- und Werkstoff 63: 327-333.

Bhat, K.M.; E.J.M. Florence. 2003. Natural Decay Resistance of Juvenile Teak Wood Grown in High Input Plantations. Holzforschung 57: 453-455.

Bhat, K.M.; P.K. Thulasidas; E.J.M. Florence; K. Jayaraman. 2005. Wood Durability of Home-Garden Teak Against Brown-rot and White-rot Fungi. Trees 19: 654-660.

Garcia, R. A.; J. de Oliveira Lopes; A.M. do Nascimento; J.V. de Figueiredo Latorraca. 2014. Color Stability of Weathered Heat-Treated Teak Wood. Maderas Ciencia y tecnología 16(4): 453-462.

Gierlinger, N.; D. Jacques; M. Grabner; R. Wimmer; M. Schwaninger; P. Rozenberg; L.E. Paques. 2004. Colour of Larch Heartwood and Relationship to Extractives and Brown-Rot Decay Resistance. Trees 18: 102-108.

Gominho, J.; J. Figueira; J.C. Rodrigues. 2001. Within-tree Variation of Heartwood, Extractives and Wood Density in the Eucalypt Hybrid Urograndis. Wood and Fiber Science 33: 3-8.

Haupt, M.; H. Leithoff; D. Meier; J. Puls; H.G. Richter; O. Faix. 2003. Heartwood Extractives and Natural Durability of Plantation-Grown Teak Wood *(Tectona grandis* L.f) – A case study. Holz als Roh- und Werkstoff. 61: 473-474.

Ismayati, M.; A. Nakagawa-Izumi; N.N. Kamaluddin; H. Ohi. 2016. Toxicity and Feeding Deterrent Effect of 2-Methylanthraquinone from the Wood Extractives of *Tectona grandis* on the Subterranean Termites *Coptotermes formosanus* and *Reticulitermes speratus*. Insects 7: 63

Kokutse, A.D.; A. Stokes; H. Bailleres; K. Kokou; C. Baudasse. 2006. Decay Resistance of Togolese teak *(Tectona grandis* L.f.) Heartwood and Relationship with Colour. Trees. 20: 219-223.

Lukmandaru, G.; K. Takahashi. 2008. Variation in the Natural Termite Resistance of Teak *(Tectona grandis L. f.)* Wood as a Function of Tree Age. Annals of Forest Science 65(7): 708p1-8

Lukmandaru, G.; K. Takahashi. 2009. Radial Distribution of Quinones in Plantation Teak (*Tectona grandis* L.f.). Annals of Forest Science 66(6): 605p1-p9.

Lukmandaru, G. 2009a. Sifat Kimia dan Warna Kayu Teras Jati pada Tiga Umur Berbeda. Jurnal Ilmu Teknologi Kayu Tropis. 7(1): 1-7.

Lukmandaru, G. 2009b. Pengukuran Kadar Ekstraktif dan Sifat Warna pada Kayu Teras Jati Doreng *(Tectona grandis)*. Jurnal Ilmu Kehutanan 3(2): 67-73.

Lukmandaru G. 2013. The Natural Termite Resistance of Teak Wood Grown in Community Forest. Jurnal Ilmu dan Teknologi Kayu Tropis 11(2): 131-139.

Lukmandaru, G. 2010. Sifat Kimia Kayu Jati *(Tectona grandis)* pada Laju Pertumbuhan Berbeda. Jurnal Ilmu dan Teknologi Kayu Tropis. 8(2): 188-196.

Lukmandaru, G. 2011. Variability in the Natural Termite Resistance of Plantation Teak Wood and its Relations with Wood Extractive Content and Color Properties. Journal Forest Research 8(1): 17-31.

Lukmandaru, G. 2016. Hubungan antara Kadar Ekstraktif dengan Sifat Warna pada Kayu Teras Jati. Jurnal Penelitian Hasil Hutan 34(3): 207-216.

Lukmandaru, G.; P. Manalu, T. Listyanto; D. Irawati; R. Pujiarti; F. Hidayati; D. Rodiana. 2016. Chemical Properties of 15-year-old Teak (*Tectona grandis* L.f) from Different Seed Sources. Wood Research Journal 7(1): 6-12.

Lukmandaru, G.; I.G.N. Sayudha. 2019. Colour Properties and Extractive Content in Young Teak Woods. Proceeding of the 9th International Symposium of Indonesian Wood Research Society. Denpasar. 26-27 September 2017, p. 164-174.

Moya, R.; A. Berrocal. 2014. A Review of Heartwood Properties of *Tectona grandis* Trees from Fast-Growth Plantations. Wood Science and Technology 48: 411-433.

Neverova, N.A.; A.A. Levchuk; L.A. Ostroukhova; E.N. Medvedeva; N.A. Onuchina; V.A. Babkin. 2013. Distribution of Extractive Substances in Wood of the Siberian Larch *(Larix sibirica* Ledeb.). Russian Journal of Bioorganic Chemistry 39(7): 712-719.

Niamke, F.B.; N. Amusant; J.P. Charpentier; G. Chaix; Y. Baissac; N. Boutahar; A.A. Adima; S. Kati-Coulibaly; C. Jay-Allemand. 2011. Relationships between Biochemical Attributes (Non-Structural Carbohydrates and Phenolics) and Natural Durability against Fungi in Dry Teak Wood *(Tectona grandis L.f.).* Annals of Forest Science 68: 201-21.

Niamké, F,B.; N. Amusant; D. Stien; G. Chaix; Y. Lozano; A.A. Kadio; N. Lemenager; D. Goh; A. A.A. Adima; S. Kati-Coulibaly, C. Jay-Allemand. 2012. 4',5'-Dihydroxy-epiisocatalponol, a new naphthoquinone from *Tectona grandis* L. f. heartwood, and fungicidal activity. International Biodeterioration & Biodegradation 74: 93-98.

Thulasidas, P.K.; K.M. Bhat. 2007. Chemical extractive compounds determining the brown-rot decay resistance of teak wood. Holz als Roh-und Werkstoff 65: 121-124.

Windeisen, E.; A. Klassen; G. Wegener. 2003. On the Chemical Characterization of Plantation Teakwood from Panama. Holzs als Roh und Werkstoff 61(6): 416-418.

Yamamoto, K.; H.M. Simatupang; R. Hashim. 1998. Caoutchouc in Teak Wood (*Tectona grandis* L.f.): Formation, Location, Influence on Sunlight Irradiation, Hydrophobicity, and Decay Resistance. Holzs als Roh und Werkstoff 56: 201–209.

Yunanta, R.R.K.; G. Lukmandaru; A. Fernandes. 2014. Sifat Kimia dan Kayu *Shorea retusa, Shorea macroptera,* dan *Shorea macrophylla.* Jurnal Penelitian Ekosistem Dipterokarpa 8(1): 15-24.

Zulkahfi; D. Irawati; T. Listyanto; D. Rodiana; G. Lukmandaru. 2020. Kadar Ekstraktif dan Sifat Warna Kayu Jati Plus Perhutani Umur 11 Tahun dari KPH Ngawi. Jurnal Ilmu Kehutanan 19(2): 213-227.

Ganis Lukmandaru, Alfian Nur Falaah, Tomy Listyanto
Department of Forest Products Technology,
Faculty of Forestry, Gadjah Mada University
Jl. Agro, Bulaksumur, Sleman, Yogyakarta
Tel. : +62-274-512102
Fax. : +62-275-550542
E-mail : glukmandaru@ugm.ac.id

Dian Rodiana
Research and Development Center, Perhutani, Central
Java, 58203, Indonesia

Catalytic Process in Producing Green Aromatics through Fast Pyrolysis of Wood of Five Tropical Fast Growing Trees Species

Joko Sulistyo, Toshimitsu Hata, Ganis Lukmandaru, Yunida Syafriani, and Sensho Honma

Abstract

The generation of liquid fuels and chemicals is potential through a catalytic fast pyrolysis (CFP) which is a rapid, inexpensive, and promising method utilizing tropical wood biomass as starting material. There is a little known in the potential of wood biomass from tropical fast-growing trees as starting materials for the production of liquid fuel and chemicals. The pyrolysis of five species (balsa, eucalyptus, jabon, mangium, and sengon) was performed with a single-shot mode pyrolyzer. In this study the formation of aromatics by pyrolytic-gas chromatography/mass spectroscopy (Py-GC/MS) is evaluated on the effect of wood species with different characteristics and its cellulose component to the formation of aromatics. ZSM-5 zeolite catalyst was used to evaluate aromatic production on balsa and ecualyptus samples. Fast pyrolysis of eucalyptus wood characterized with low content of ash and high percentages of hollocellulose and α-cellulose produced much high relative peaks of levoglucosan and small relative peaks of lignin derived products. Meanwhile high content of vollatile matter and high crystallinity of cellulose attributed balsa and jabon woods as feedstock for fast pyrolysis. The catalytic process in fast pyrolysis of eucalyptus decomposed the most of oxygenated compound such as levoglucosan and furfural into aromatics in the presence of ZSM-5. Coke formation on the surface catalyst might lead partly of decomposition of levoglucosan and furfural to form aromatics in the catalytic fast pyrolysis of balsa wood. Cellulose component was determined on the formation of benzene, toluene, styrene, p-xylene, indane, indene, and naphthalene in catalytic fast pyrolysis of wood.

Keywords: aromatics, catalytic fast pyrolysis, Py-GC/MS, wood characteristics, ZSM-5 catalyst.

Introduction

The production of fuels and chemicals from renewable resources is currently generating new interest. In contrast to fossil fuels, the use of renewable resources such as biomass for energy provides significant environmental advantages. Woody biomass which is available in a large amount in many parts of the world especially in tropical area is potential starting materials for liquid fuel and chemicals. One of the woody biomass sources is from the harvesting of industrial plantation and community forests which is mainly composed of fast-growing tree species. Renewable biomass has the potential to generate inexpensive fuels and organic chemicals if they are efficiently converted via an appropriate processing route. Therefore, clean energy development could turn away from fossil fuel towards regenerative energy sources such as wood biomass.

Fast pyrolysis thermal decomposition of biomass feedstock using a relatively high heating rate can yield liquids of up to 70~75% of the weight of the starting material (Gurgens *et al*. 2014). The crude pyrolysis liquid product is potential energy product because of its high energy density (Bridgwater 1996). However, the pyrolytic oil product requires full deoxygenation which can be accomplished by hydro-treating and catalytic vapor cracking (Czernik and Bridgwater 2004) and also by catalytic upgrading (Vitolo *et al.* 2001) to obtain a conventional transport fuels. Carlson *et al.* (2009) have developed a single step catalytic fast pyrolysis to produce aromatics including benzene, toluene, and naphthalene from biomass in a single reactor with a short residence time. The aromatic production and selectivity are found as a function of catalyst to feedstock weight ratio, heating rate, and reaction temperature (Carlson *et al*. 2010). French and Czernik (2010) performed a study on the efficiency of various catalyst for aromatic production and found that the highest yield of aromatics from wood, around 16 wt% including 3.5 wt% of toluene were obtained by ZSM-5 zeolite catalyst. Mihalcik *et al*. (2011) screened acidic zeolites for catalytic fast pyrolysis of biomass and its components and found that H-ZSM-5 zeolite lead to an increased production of aromatic hydrocarbons. Besides improving the quality of bio oil, impregnation of 10 wt% Fe to ZSM-5 can increase in the amount of phenolic compound, aromatic and aliphatic hydrocarbon (Saracoglu *et al.* 2017).

There is less study on the development of liquid fuel and aromatics production through the catalytic fast pyrolysis utilizing wood biomass from tropical fast growing trees as starting material. In a previous study, it was found that aromatics including benzene, toluene, styrene, naphthalenes, and indanes were formed by a catalytic fast pyrolysis of red meranti (*Shorea leprosula*) biomass (Sulistyo *et al.* 2013). Since there are many fast-growing trees available in tropical area with different characteristics of wood, so selection of the potential woody biomass and cellulose component as starting material is useful. The objective of the study is to use Py-GC/MS to evaluate five tropical wood species and their cellulose components against ZSM-5 catalysts to determine relative abilities to deoxygenated pyrolytic condensable components and produce aromatics.

Materials and Methods

A wood disc sample was collected from the bottom part of trees of jabon (*Antocephalus cadamba*), sengon (*Paraserianthes mollucana*), and balsa (*Ochroma* sp) grown in community forest managed by PT. Partawood in Probolinggo – East Java Province, Indonesia. The present study used three trees for each wood species. Two other wood species i.e. mangium (*Acacia mangium*) and eucalyptus (*Eucalyptus pellita*) grown in Wanagama experimental forest of Universitas Gadjah Mada in Gunung Kidul District - Yogyakarta were used without replication. Part of the wood disc sample was milled into powder and sieved with wire mesh screens to obtain particles with size range of 0.25 ~ 0.42 mm (passing through 40 mesh sieve and retained by 60 mesh sieve). ZSM-5 catalyst (Zeolyst International, CVB 3024E, nominal cation form: ammonium) was used in this study.

The moisture and volatile contents were determined by a gravimetric method according to ASTM D2867-17 and D1762-64, respectively. For moisture content, the sample was heated at 105 °C for 2 h in the oven. The sample for volatile matter was heated to 950 °C for 7 min in muffle furnace. The ash content was obtained by heating the samples at 600 °C for 1 h in air to constant weight in muffle furnace according to ASTM D2866-94, the fixed carbon content was estimated by difference as follows :

Fixed carbon content (%) = [100 - (% ash content + % volatile matter content)] ....(1)

For determining of holocellulose and α-cellulose contents, wood powder equal to dry weight of 2 g was determined according to chlorite acid method (Browning 1967) and ASTM D1103-60, respectively. The hemicellulose content was determined by substraction. Extractive soluble in alcohol-toluene was determined according to ASTM D1107-96. The crystallinity level of the wood sawdust were measured with an X-ray diffractometer (Shimadzu MAXima XRD 7000) for wide angle X-Ray Difraction (XRD). The equipment settings were 40 mA and 30 kV with a Cu K_α radiation wavelength of 1.54 Å. The receiving slits were 0.3 mm, and the intensity was measured as a function of the scattering angle 2θ by θ-2θ scan. The angle range was 10-40 degrees and the step was 0.02 degree. The measuring time was chosen so the maximum intensity was about 84 counts, and it was typically 0.60s per point. The crystallinity profiles of the wood sawdust are explained in terms of wood sawdust content. Crystallinity Index (CI) is calculated as the ratio between the area of the crystalline contribution and the total area according to equation:

$$CI\ (\%) = [(I_{002} - I_{am}) / I_{002}] \times 100 \quad (2)$$

where I_{002} is the diffraction peak intensity of the (002) plane, I_{am} is the amorphous part of diffraction intensitylocated at 2θ between 18°–19°.

The pyrolysis of wood (0.05 mg) was performed with a single-shot mode pyrolyzer (PY-2020, Frontier Lab.) directly interfaced to a GC/MS system Shimadzu (QP-5000) equipped with DB - 5HT capillary column with a length of 30 m × diameter of 0.250 mm (Agilent Technologies). The effect of catalyst was evaluated on balsa and eucalyptus only. Wood meal and catalyst powder were mixed in a 1 (balsa or eucalyptus wood) : 9 (ZSM-5) (0.5 mg) or 1 (balsa cellulose or eucalyptus cellulose) : 9 (ZSM-5) (0.5 mg) ratio. The interface temperature was set to 310 °C. The mass spectra of samples were then compared to values in NIST library and literatures. The relative area percentage was expressed as percentages obtained by a computerized integrator based on the peak area from total ion chromatography.

The fast pyrolysis was performed by raising the temperature of pyrolyzer furnace to 600 °C without heating the sample. When the condition had stabilized, then the sample in steel sampling cup, 5 mm in diameter and 7 mm in height, was dropped to the furnace and kept at 600 °C for 0.2 min under the He gas flow rate of 50 ml/min. The column temperature was set to 70 °C and the injection temperature was 320 °C with a flow pressure of 1000 °C kPa. The oven temperature was held at 90 °C for 3 min and then increased up to 190 °C at 10 °C/min and kept for 5 min. The temperature increased from 190 °C to 320 °C at 10 °C/min and isothermal at 320 °C for 35 min. The carrier gas used was helium with a controlled flow of 50 ml/min. The data was analyzed using one way analysis of variance (ANOVA) followed by Tukey test ($p = 0.05$). All statistical calculations were conducted using SPSS-Win 16.0.

Results and Discussion

Chemical Characteristics

Table 1 shows the proximate analysis of wood of five potential fast growing species. All wood species possessed high volatile contents, on the other hand showing a low content of fixed carbon and ash content that is comparable with Meincken and Tyhoda (2014). Analysis of variance showed that there is no significant differences on the volatile matters, fixed carbon, and ash contents of jabon, sengon, and balsa. The volatile contents of jabon, sengon and balsa woods are higher than that of eucalyptus and that of rockrose wood reported by Gomez-Serrano *et al.* (1993). Eucalyptus wood contained lesser ash than those of jabon, sengon, and balsa woods. It is expected that slight ash content in eucalyptus wood influences on the high in yields of anhydro-sugars and high molecular furan and pyran products and also on the slight in the yield of lignin derived products such as vinyl guaiacol and syringol (Azeez *et al.* 2011). Strezov *et al.* (2007) reported that sugar pine wood containing 80.7% of volatile matter through a pyrolysis at temperature of 500 and 900 °C with a heating rate of 50 °C/min yielded a double gaseous product than that of bagasse and macadamia nut shell containing volatile matter of 72.7% and 72.6%, respectively. The different content of volatile matters in different wood species supposed to influence on the formation of aromatics from a catalytic fast pyrolysis process.

Table 2 shows the significant differences at 0.01 levels in the hollocellulose, α-cellulose, hemicellulose and extractive soluble in alcohol-toluene contents in jabon, sengon and balsa. Mangium dan eucalyptus woods possessed higher content of holocellulose and α-cellulose but lower content of extractive than those of jabon, sengon and balsa. In thermochemical decomposition, cellulose degraded into anhidrocellulose and levoglucosan, meanwhile hemicellulose degraded mostly into volatile matter (Mohan *et al.* 2006). Sharma *et al.* (2015) emphasized that cellulose and hemicellulose components produce more volatile and gas products, while lignin predominantly forms a charred residue. Therefore mangium and eucalyptus woods were potential to be used in fast pyrolysis for aromatic production. Jabon and balsa woods with high content of hemicellulose 30.9% and 34.6%, respectively, were reasonable to yield high volatile matter contents of 92.2% and 95.0%, respectively as shown in Table 1.

Table 1. Proximate analysis of the wood of five potential fast growing trees.

	Proximate analysis (wt.%, dry basis)		
Species	Volatile matter	Fixed carbon	Ash
Mangium (*Acacia mangium*)	-	-	-
Ekaliptus (*Eucalyptus pellita*)	82.6	16.94	0.41
Jabon (*Antocephalus cadamba*)	93.2	5.33	2.13
Sengon (*Paraserianthes mollucana*)	89.8	8.85	1.34
Balsa (*Ochroma sp.*)	95.0	3.16	1.85

Remark: jabon, sengon and balsa showed no significantly different; (-) : not determined

Table 2. Chemical components of the wood of five potential fast growing trees

	Components analysis (wt%, dry basis)			
Species	Holocellulose	α-cellulose	Hemicellulose	Extractive
Mangium (*Acacia mangium*)	87.7	54.7	33.0	12.1
Ekaliptus (*Eucalyptus pellita*)	81.8	56.1	25.7	11.2
Jabon (*Antocephalus cadamba*)	72.9^a	42.0^a	30.9^b	14.1
Sengon (*Paraserianthes mollucana*)	77.9^b	51.5^b	26.5^a	16.3
Balsa (*Ochroma sp.*)	78.4^b	43.9^a	34.6^c	14.2

Remark: values followed by the same letter on the same column are not significantly different at 0.01 level (Tukey test). Extractive soluble in alcohol-toluene.

Crystallinity Characteristics

Figure 1 shows the X-ray diffractogram of the wood samples studied. There are two major diffraction peaks at approximately 16° and 22° comparable with Poletto *et al.* (2012). The peak intensities differ from one species to another. The clearer difference occurred at the peak range between 21.80° and 22.66° 2θ reflection. The peak area at 21.80~22.66° 2θ reflection follow the sequence mangium > eucalyptus > sengon > balsa > jabon, as can be seen in Figure 1.

The crystallinity of five wood using XRD varied from 26% to 41%. The highest crystallinity was mangium (41.37%), then followed by balsa (34.2%), sengon (33.6%), jabon (33%), and the lowest was eucalyptus (26.2%). The comparatively high level of lignin content along with crystalinity index in mangium wood is not expected. The reason might be due to the large amount of crystalline regions present in cellulose. In addition, these results are corresponding with Poletto *et al.* (2012) that the eucalyptus crystallinity was lower than other wood. The differences are influenced by the crystallite size along the crystallographic planes. The crystallinity index increased with increasing crystallite size because the crystallite surface corresponding to the amorphous cellulose region reduced (Kim *et al.* 2010; Poletto *et al.* 2012).

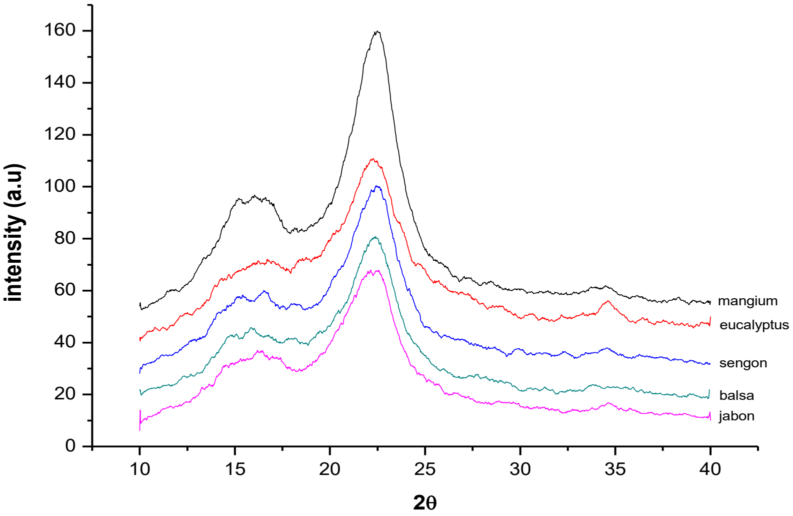

Figure 1. X-ray diffractograms of five wood species.

Non-Catalytic Fast Pyrolysis

Figure 2 display the ion chromatograms from non-catalytic fast pyrolysis of wood of the five potential fast growing species. Non-catalytic fast pyrolysis mangium, eucalyptus, balsa, jabon, and sengon woods at 600 °C formed vapours which was analyzed with GC/MS using DB - 5HT column showing major peaks of hydroxyl acetaldehyde, furfural, guaiacol, 4-methylguaiacol, 4-vinylguaiacol, syringol, levoglucosan, vinylsyringol, and acetoyringon (Tsuge *et al.* 2011).

Fast pyrolysis increased the decomposition of wood through rapid and simultaneous depolymerizing and fragmenting of cellulose, hemicellulose, and lignin with rapid increase in temperature (Mohan *et al.* 2006). Under fast pyrolysis at 600 °C, cellulose depolymerizes to miscellaneous oxygenated fragments such as hydoxyacetaldehyde, furfural, and levoglucosan, at retention time of 7.49, 9.25 and 11.97 min, respectively. Lignin depolymerized to guaiacol, 4-methylguaiacol, 4-vinylguaiacol, and syringol, at retention time of 9.73, 10.3, 10.8 and 11.2 min respectively (Shen and Gu 2009; Azeez *et al.* 2010; Boateng *et al.* 2010). The relative major peaks of chromatogram of non-catalytic fast pyrolysis are shown in Table 3. The relative peaks of levoglucosan from non-catalytic fast pyrolysis of eucalyptus wood much higher than other peaks including furfural, 4-vinylguaiacol, vinylsyringol, and acetosyringon. The high content of α-cellulose and a small content of ash in eucalyptus wood, as shown in Table 1 and 2, might influence on the high relative peak of levoglucosan, as the yield of levoglucosan is affected by the source of the cellulose (Azeez *et al*. 2011). The small content of ash in eucalyptus wood might also play an important role in producing a slight yield of lignin derived products such as guaiacol, 4-methylguaiacol, syringol and acetosyringon (Azeez *et al.* 2011). The relation of small ash content to the promoting of high yield of levoglucosan from the low crystallinity of eucalyptus wood were opposite with the previous finding that cellulose with high crystallinity degree tends to produce levoglucosan in a higher yield during cellulose pyrolysis (Wang *et al.* 2013; Jiang *et al.* 2016; Zheng *et al.* 2016). They reported that the cellulose with low crystallinity degree seems to have thermally decomposed through the formation of a liquid intermediate contained dehydration reactions. Meanwhile the relative major peaks were found on non-catalytic fast pyrolysis of balsa, jabon, and sengon woods. It is might be affected by high content of volatile matter which is came from cellulose and hemicellulose in these three wood species as shown in Table 1 and their high crystallinity of cellulose.

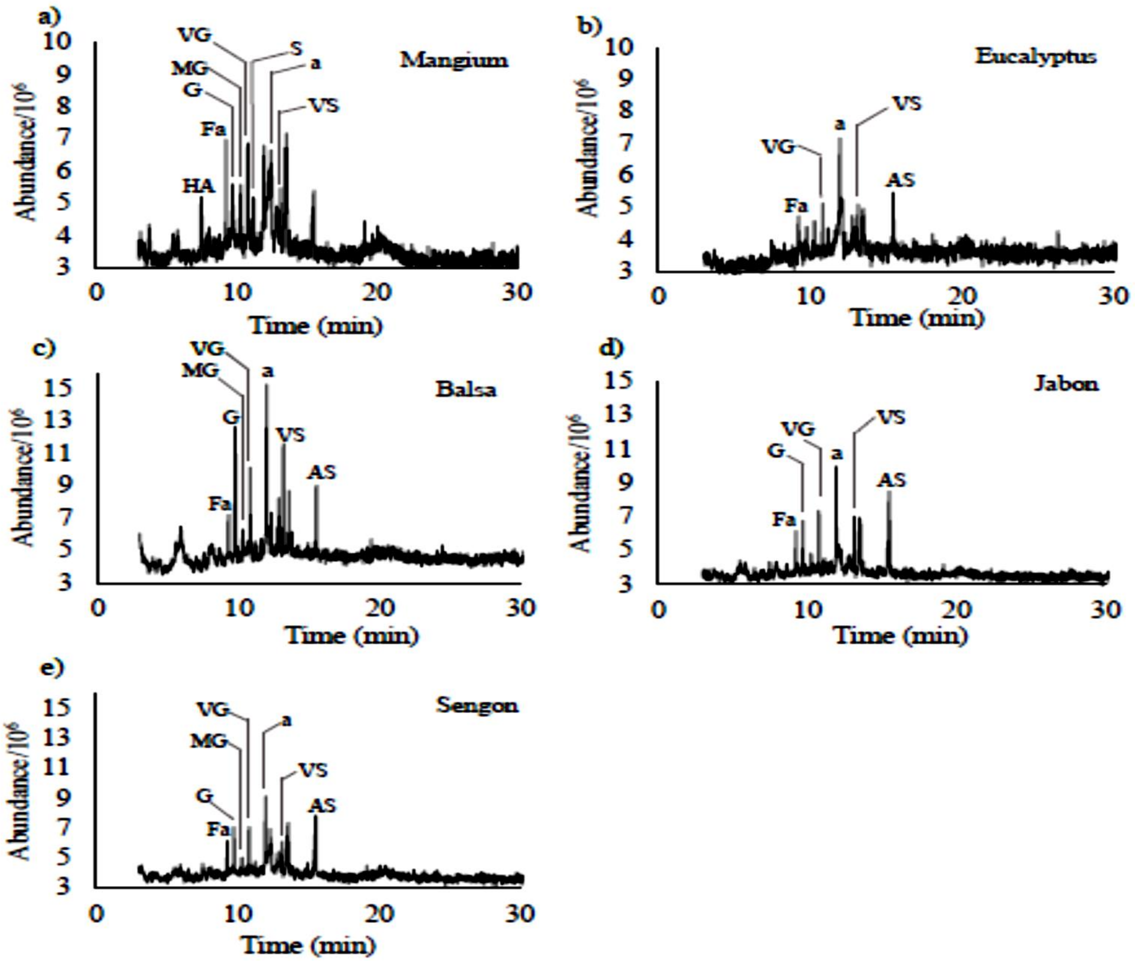

Figure 2. The ion chromatograms from non-catalytic fast pyrolysis of a) mangium, b) eucalyptus, c) balsa, d) jabon and e) sengon wood species. HA – Hydroxy acetaldehyde, Fa – Furfural, G – Guaiacol, MG – 4-Methylguaiacol, VG – 4-Vinylguaiacol, S – Syringol, a – Levoglucosan, VS – Vinylsyringol, AS – Acetosyringon.

Table 3. Relative major peaks (%) from non-catalytic fast pyrolysis of the wood of five potential fast growing trees

RT (min)	Compound	Mangium	Eucalyptus	Balsa	Jabon	Sengon
7.49	Hydroxy acetaldehyde	2.84	-	-	-	-
9.25	Furfural	13.12	9.54	6.44	8.67	6.19
9.73	Guaiacol	2.88	-	24.54	10.30	17.01
10.30	4-Methylguaiacol	4.88	-	1.47	-	0.45
10.81	4-Vinylguaiacol	4.18	7.75	7.79	0.53	6.22
11.22	Syringol	2.65	(-)	-	-	-
11.97	Levoglucosan	13.95	70.92	33.65	16.74	22.60
13.17	Vinylsyringol	16.97	10.58	11.02	8.40	10.41
15.51	Acetosyringon	-	1.21	3.10	15.04	10.30
	Unidentified	38.53	-	11.99	40.32	26.83

Remark: RT= Retention time; (-) = not detected

Catalytic Fast Pyrolysis of Wood

Figure 3 shows ion chromatogram non-catalytic and catalytic pyrolysis of eucalyptus and balsa woods. The catalytic processes in fast pyrolysis of eucalyptus and balsa wood released the aromatics peaks including benzene, toluene, styrene, p-xylene, o-xylene, indane, indene, and naphthalene, following the decreasing the relative peaks of oxygenated compounds such as furfural, guaiacol, 4-vinylguaiacol, syringol, levoglucosan, vinylsyringol and acetosyringon (Tsuge *et al.* 2011; Schultz *et al.* 2016) as shown in Table 4. Therefore catalytic fast pyrolysis decomposed carbohydrates and lignin to produce bio-oil (Mohan *et al.* 2006) containing furfural, levoglucosan, guaiacol, 4-vinylguaiacol, syringol, vinylsyringol, and acetosyringon which were then diffused into ZSM-5 pores and through a series of decarbonylation, decarboxylation, dehydration, and oligomeration reactions, aromatics were formed (Carlson *et al.* 2009) which were not detected on the non-catalytic fast pyrolysis of wood. ZSM-5 catalyst with a potential ideal pore size in the range of 0.52~0.55 nm (Mihalcik *et al.* 2011) and Brönsted acid sites (Corma *et al.* 2009) leads to the production of aromatics in this study. The mechanism of aromatic formation from carbohydrates and lignin through a catalytic fast pyrolysis was explained elsewhere (Carlson *et al*. 2009; Shen and Gu 2009; Shen *et al*. 2010).

Relative major peaks from non-catalytic and catalytic fast pyrolysis of balsa and eucalyptus wood is shown in Table 4. There is much different between relative peaks of levoglucosan and furfural from non-catalytic and catalytic fast pyrolysis of eucalyptus wood i.e. 70.9 ~ 0.98 and 9.54 ~ 1.44, respectively. Meanwhile there is lesser different between those from non-catalytic and catalytic fast pyrolysis of balsa wood i.e. 33.6 ~ 12.6 and 6.4 ~ 1.2, respectively. The catalytic process in fast pyrolysis of eucalyptus decomposed the most of oxygenated compound such as levoglucosan and furfural into aromatics in the presence of ZSM-5. The potential aromatics species formed from catalytic fast pyrolysis of eucalyptus wood were including toluene, styrene, p-xylene, o-xylene, indane, indene and naphthalene. On the other hand, it was found that partly of levoglucosan and furfural generated to form aromatics in the fast pyrolysis of balsa wood. The fast pyrolysis of balsa wood released abundance volatiles as shown in Table 1, that might be intermediate species from carbohydrate vapors (Jia *et al*. 2017). The abundance intermediate species might cause the formation of unsaturated coke on the surface of the catalyst. The coke is formed through intermediate polymers, which ultimately decompose to unsaturated coke (Carlson *et al*. 2010b). The coke formation on the external surface are responsible for deactivation of zeolites, and the coke deposition within the zeolite pore reduce the capillary and diffusion flow of reactants and finally decrease the aromatic yield (Shen *et al.* 2015; Galadima and Muraza 2015; Rahman *et al.* 2018). Therefore it might require more ZSM-5 catalyst to react with all oxygenated compounds from fast pyrolysis of balsa wood to form aromatics, as aromatics production is found as a function of catalyst to feedstock weight ratio (Carlson *et al*. 2010a).

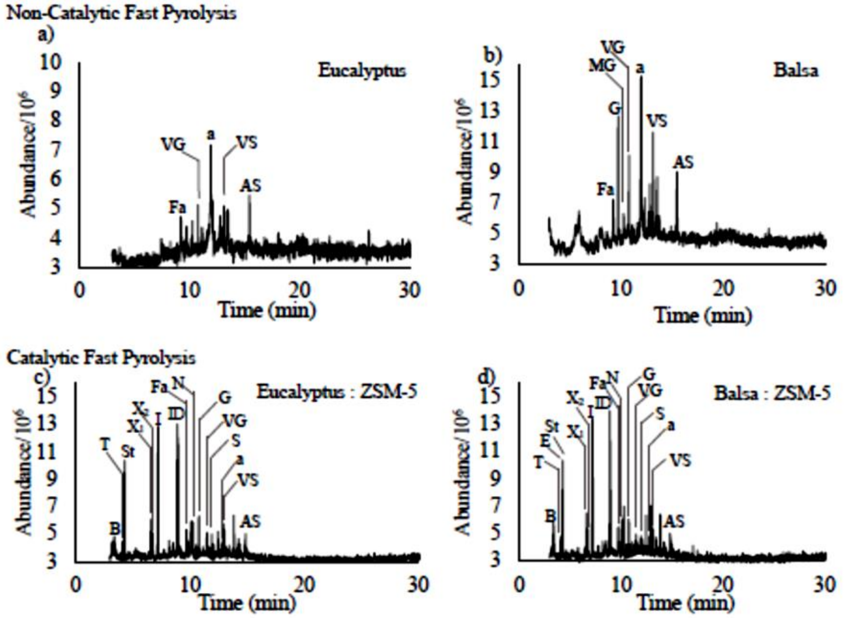

Figure 3. The ion chromatograms non-catalytic fast pyrolysis of a) eucalyptus and b) balsa woods, and catalytic fast pyrolysis of c) eucalyptus and d) balsa woods. B – Benzene, T – Toluene, St – Styrene, X_1 – P-Xylene, X_2 – O-Xylene, I – Indane, ID – Indene, Fa – Furfural, N – Naphthalene, G – Guaiacol, VG – 4-Vinylguaiacol, S – Syringol, a – Levoglucosan, VS – Vinylsyringol, AS – Acetosyringon.

Table 4. Relative major peaks (%) from non-catalytic and catalytic fast pyrolysis of balsa and eucalyptus woods.

	Balsa				Eucalyptus			
Compound	RT (min)	Non-Catal.	RT (min)	Catal.	RT (min)	Non-Catal.	RT (min)	Catal.
Benzene		-	3.42	0.78		-	3.40	0.14
Toluene		-	4.12	1.57		-	4.12	1.17
Ethylbenzene		-	4.30	12.59		-		0.01
Styrene		-	4.31	11.84		-	4.30	16.16
P-xylene		-	6.62	3.79		-	6.62	4.19
O-Xylene		-	6.73	1.83		-	6.73	1.46
Indane		-	7.23	13.43		-	7.23	19.90
Indene		-	8.94	13.19		-	8.98	21.07
Furfural	9.28	6.44	9.75	1.23	9.24	9.54	9.72	1.44
Naphthalene		-	10.13	2.48		-	10.17	2.29
Guaiacol	9.76	24.54	10.80	0.88		-	10.79	2.63
4-Methylguaiacol	10.30	1.47		-				
4-Vinylguaiacol	10.81	7.79	11.51	0.25	10.82	7.75	11.50	0.64
Syringol		-	11.96	0.25		-	11.95	0.95
Levoglucosan	11.99	33.65	12.97	12.62	11.97	70.92	12.96	0.98
Vinylsyringol	13.18	11.02	13.17	0.19	13.17	10.58	13.03	0.51
Acetosyringon	15.51	3.10	14.90	0.26	15.49	1.21	14.83	1.17
Unidentified		11.99		22.81		-		25.3

Remark: RT = Retention time; (-) = not detected

Catalytic Fast Pyrolysis of Cellulose Component

Ion chromatogram of catalytic fast pyrolysis of cellulose of eucalyptus and balsa woods is shown in Figure 4. Relative major peaks from catalytic fast pyrolysis of cellulose of eucalyptus and balsa woods are presented in Table 5. Catalytic fast pyrolysis of both celluloses of eucalyptus and balsa woods released major peaks of aromatics including benzene, styrene, p-xylene, indane, indene, and naphthalene along with the disappearing oxygenated compound derivates of cellulose i.e. furfural and levoglucosan (Tsuge *et al.* 2011). The catalytic process decomposed all cellulose derivates from fast pyrolysis of cellulose of eucalyptus wood to form aromatics. On the other hand, partly cellulose derivates of cellulose of balsa wood were degraded to form aromatics. As discussed previously, the formation of unsaturated coke from abundance intermediate species on the surface of ZSM-5 catalyst influenced on the deactivation of the catalyst (Carlson *et al.* 2010b; Jia *et al.* 2017). Deactivation of ZSM-5 catalyst might determine the partial degradation of cellulose of balsa wood. The abundance vapor products from fast pyrolysis of balsa wood, corresponding to the high volatile matter content of balsa wood in Table 1, might require more availability of ZSM-5 catalyst.

Selectivity distribution of aromatics from catalytic fast pyrolysis of cellulose of eucalyptus wood from were styrene > indene > p-xylene = indane > benzene. Meanwhile cellulose of balsa wood released aromatics with the selectivity distribution was from indane > indene > styrene > benzene > p-xylene > o-xylene > naphthalene > toluene that was similar with the selectivity distribution from catalytic fast pyrolysis of balsa wood.

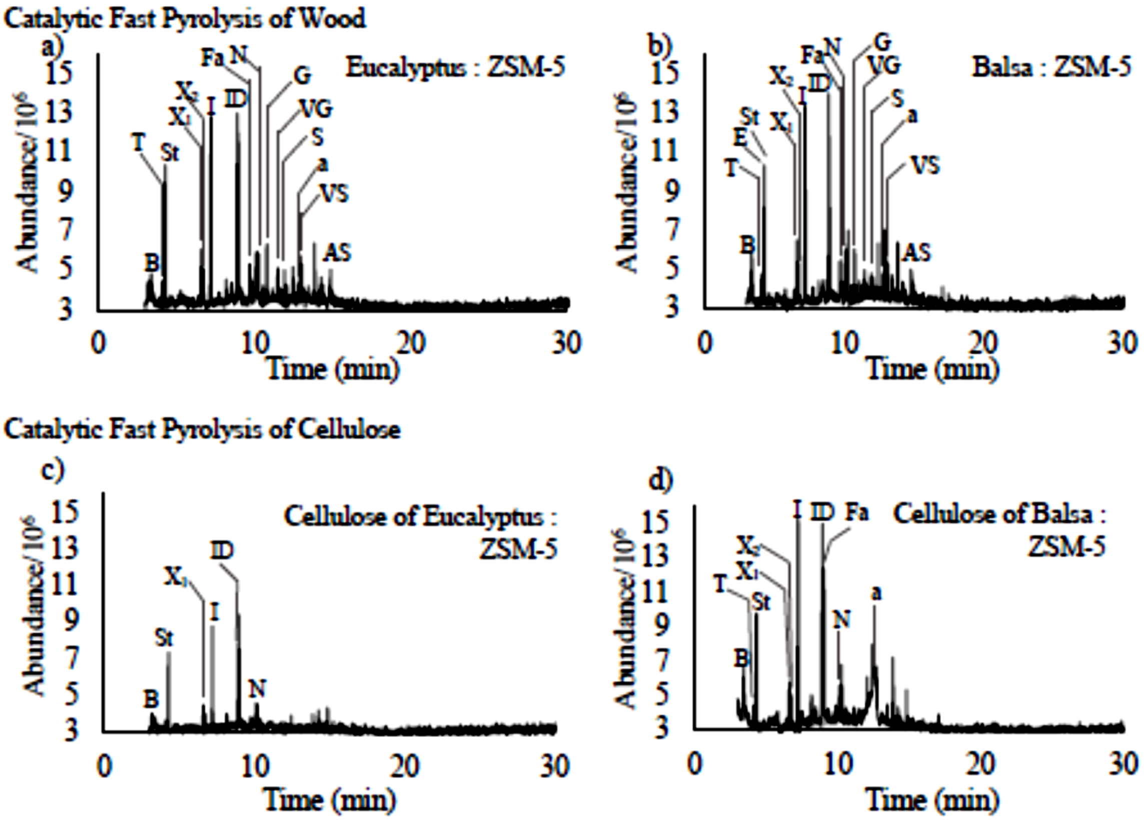

Figure 4. The ion chromatograms catalytic fast pyrolysis of a) eucalyptus and b) balsa wood, and cellulose of c) eucalyptus and d) balsa wood species. The meaning of peak is the same as that in Figure 3.

Table 5. Relative major peaks (%) from catalytic fast pyrolysis of wood and cellulose of balsa and eucalyptus woods.

Compound	Balsa		Eucalyptus	
	Wood	Cellulose	Wood	Cellulose
Benzene	0.78	3.15	0.14	0.21
Toluene	1.57	0.95	1.17	-
Ethylbenzene	12.59	-	0.00	-
Styrene	11.84	10.90	16.16	24.14
P-xylene	3.79	2.05	4.19	2.83
O-xylene	1.83	1.72	1.46	-
Indane	13.43	17.65	19.90	2.83
Indene	13.19	13.08	21.07	11.55
Furfural	1.23	3.69	1.44	-
Naphthalene	2.48	1.23	2.29	6.42
Guaiacol	0.88	-	2.63	-
4-Methylguaiacol	-	-	0.00	-
4-Vinylguaiacol	0.25	-	0.64	-
Syringol	0.25	-	0.95	-
Levoglucosan	12.62	9.30	0.98	-
Vinylsyringol	0.19	-	0.51	-
Acetosyringon	0.26	-	1.17	-
Unidentified	22.81	36.28	25.30	52.02

Remark: (-) = not detected

Conclusions

Fast pyrolysis of eucalyptus wood characterized with low content of ash and high percentages of hollocellulose and α-cellulose produced much high relative peaks of levoglucosan followed by furfural and also small relative peaks of lignin derived products. Meanwhile high content of vollatile matter and high crystallinity of cellulose attributed balsa and jabon woods in fast pyrolysis. The catalytic processes in fast pyrolysis of eucalyptus and balsa wood released the aromatics peaks including benzene, toluene, styrene, p-xylene, o-xylene, indane, indene, and naphthalene, following the decreasing the relative peaks of oxygenated compounds such as furfural, guaiacol, 4-vinylguaiacol, syringol, levoglucosan, vinylsyringol and acetosyringon. The catalytic process in fast pyrolysis of eucalyptus decomposed the most of oxygenated compound such as levoglucosan and furfural into aromatics in the presence of ZSM-5. In contrary, coke formation on the surface catalyst might cause partly of decomposition of levoglucosan and furfural to form aromatics in the catalytic fast pyrolysis of balsa wood. Cellulose component was determined on the formation of benzene, toluene, styrene, p-xylene, indane, indene, and naphthalene in catalytic fast pyrolysis of wood.

Acknowledgement

This research was carried out with support from Grant in-Aid for International Research Collaboration and Scientific Publication from Directorate General for Higher Education – Ministry of Education fiscal year 2015.

References

ASTM. 1977. ASTM D1103-60. Method of test for alpha-cellulose in wood. Annual Book of ASTM Standards. Philadelphia.

ASTM. 1984. ASTM D1762. Standard test method for chemical analysis of wood charcoal. Annual Book of ASTM Standards. Philadelphia.

ASTM International. 2002. ASTM D1107-96. Standard test methods for ethanol-toluene solubility of wood. Annual Book of ASTM Standards. Section Four Construction Volume 04.10 Wood. Philadelphia.

ASTM International. 2004. ASTM D2866-94. Standard test method for total ash content of activated carbon. ASTM, Philadelphia.

ASTM International. 2017. ASTM D2867-17. Standard test methods for moisture in activated carbon. ASTM, Philadelphia

Azeez, A.M.; D. Meier; J. Odermatt; T. Willner. 2010. Fast pyrolysis of African and European lignocellulosic biomasses using Py-GC/MS and fluidized bed reactor. Energy and Fuels 24: 2078-2085.

Azeez, A.M.; D. Meier; J. Odermatt. 2011. Temperature dependence of fast pyrolysis volatile products from European and African biomass. Journal of Analytical and Applied Pyrolysis 90: 81-92.Boateng, A.A.; C.A. Mullen; C.M. McMahan; M.C. Whalen; K. Cornish. 2010. Guayule (*Parthenium argentatum*) pyrolysis and analysis by Py-GC/MS. Journal of Analytical and Applied Pyrolysis 87: 14-23.

Bridgwater, A.V. 1996. Production of high grade fuels and chemicals from catalytic pyrolysis of biomass. Catalysis Today 29: 285-295.

Browning BL. 1967. Methods of wood chemistry. Volumes I & II. John Wiley & Sons. USA.

Carlson, T.R.; G.A. Tompsett; W.C. Conner; G.W. Huber. 2009. Aromatic production from catalytic fast pyrolysis of biomass-derived feedstocks. Topics in Catalysis 52: 241-252.

Carlson, T.R.; J. Jae; Y. Lin; G.A. Tompsett; Huber GW. 2010a. Catalytic fast pyrolysis of glucose with HZSM-5: The combined homogeneous and heterogenous reactions. Journal of Catalysis 270: 110-124.

Carlson, T.R.; J. Jungho; L. Yu-Chuan; A.T. Geoffrey; W.H. George. 2010b. Catalytic fast pyrolysis of glucose with HZSM-5: The combined homogeneous and heterogeneous reactions. Journal of Catalysis 270: 110-124.

Corma, A.; F.J. Llopis; C. Martinez; G. Sastre; S. Valencia 2009. The benefit of multipore zeolite: Catalytic behavior of zeolites with intersecting channels of different sizes for alkylation reactions. Journal of Catalysis 268: 9-17.

Czernik, S.; A.V. Bridgwater. 2004. Overview of applications of biomass fast pyrolysis oil. Energy and Fuel 18: 590-598.

French, R.; S. Czernik. 2010. Catalytic pyrolysis of biomass for biofuels production. Fuel Processing Technology 91: 25-32.

Galadima, A.; O. Muraza 2015. In situ fast pyrolysis of biomass with zeolite catalysts for bioaromatics/gasoline production: a review. Energy Conversy Management 105: 338-354.

Gomez-Serrano, V.; C. Valenzuela-Calahorro; J. Pastor-Villegas 1993. Characterization of rockrose wood, char and activated carbon. Biomass and Bioenergy 4: 355-364.

Gurgens. J.F.; M. Carrier; M.P. Garcia-Aparicio. 2014. Biomass conversion to bioenergy products. In Bioenergy from wood: Sustainable production in the tropics. Chapter 7. Ed. T. Seifert. Springer Science-Bussiness Media. Dordrecht.

Jia, L.Y.; M.Raad; S. Hamieh; J. Toufaily; T. Hamieh; M. Bettahar; G. Mauviel; M. Tarrighi; L. Pinard; A. Dufour. 2017. Catalytic fast pyrolysis of biomass: superior selectivity of hierarchical zeolites to aromatics. Green Chemistry 19: 5442-5459.

Jiang, L.Q.; A.Q. Zheng; Z.L. Zhao; F. He; H.B. Li; N.N. Wu. 2016. The comparison of obtaining fermentable sugars from cellulose by enzymatic hydrolysis and fast pyrolysis. Bioresources Technology 200: 8-13.

Kim, S.S.; J. Kim; Y.H. Park; Y.K. Park. 2010. Pyrolysis kinetics and decomposition characteristics of pine trees. Bioresources Technology 101 : 9797-9802.

Meincken, M.; L. Tyhoda. 2014. Biomass quality. In Bioenergy from wood: Sustainable production in the tropics, Chapt. 8. Ed. Seifert T. Springer. Dordrecht.

Mihalcik, D.J., C.A. Mullen; A.A. Boateng. 2011. Screening acidic zeolites for catalytic fast pyrolysis of biomass and its components. Journal of Analytical and Applied Pyrolysis 92: 224-232.

Mohan, D.; C.U. Pittman Jr, P.H. Steele. 2006. Pyrolysis of wood/biomass for bio-oil: A critical review. Energy and Fuels 20: 848-889.

Saracoglu, E.; B.U. Basak; A.V. Esin 2017. Upgrading of fast pyrolysis bio-oil over Fe modified ZSM-5 catalyst to enhance the formation of phenolic compounds. International Journal of Hydrogen Energy 30: 1-11.

Poletto, M.; J.Z. Ademir; M.C.F. Maria; M.C.S. Ruth. 2012. Thermal decomposition of wood: Influence of wood components and cellulose crystallite size. Bioresources Technology 109 : 148-153.

Rahman, M.M., L. Ronghou, C. Junmeg. 2018. Catalytic fast pyrolysis of biomass over zeolites for high quality bio-oil: a review. Fuel Processing Technology 180: 32-46.

Sharma, A.; V. Pareek; D. Zhang. 2015. Biomass pyrolysis – A review of modelling, process parameters and catalytic studies renewable and sustainable. Energy Reviews 50: 1081-1096.

Schultz, E.L.; A.M. Charles; A.B. Akwasi. 2016. Aromatic hydrocarbon production from *Eucalyptus urophylla* pyrolysis over several metal-modified ZSM-5 catalyst. Energy Technology 4: 1-10.

Shen, D.K.; S. Gu. 2009. The mechanism for thermal decomposition of cellulose and its main products. Bioresource Technology 100: 6496-6504.

Shen, D.K.; S. Gu; A.V. Bridgwater. 2010. Study on the pyrolytic behaviour of xylan-based hemicellulose using TG-FTIR and Py-GC-FTIR. Journal of Analytical and Applied Pyrolysis 87: 199-206.

Shen, D.; J. Zhao; R. Xiao; S. Gu 2015. Production of aromatic monomers from catalytic pyrolysis of black-liquor lignin, Journal of Analytical and Appled Pyrolysis 111: 47-54.

Strezov, V.; M. Patterson; V. Zymla; K. Fisher; T.J. Evans; P.F. Nelson. 2007. Fundamental aspects of biomass carbonisation. Journal of Analytical and Applied Pyrolysis 79: 91-100.

Sulistyo, J.; T, Hata; S. Honma; R. Asakura; S.N. Marsoem. 2013. Green aromatics from catalytic fast pyrolysis of fast-growing meranti biomass. Wood Research Journal 40: 13-18.

Tsuge, S.; H. Ohtani; C. Watanabe. 2011. Pyrolysis-GC/MS data book of synthetic polymers. Pyrograms, thermograms and MS of pyrolyzates. Elsevier. UK.

Vitolo, S.; B. Bresci; M. Seggiani; M.G. Gallo. 2001. Catalytic upgrading of pyrolytic oils over HZSM-5 Zeolite: Behaviour of the catalyst when used in repeated upgrading-regenerating cycles. Fuels 80: 17-26.

Wang, Z.; A.G. McDonald; R.J. Westerhof; S.R. Kersten; C.M. Cuba-Torres; S. Ha; B. Pechad; M. Garcia-Perez. 2013. Effect of cellulose crystallinity on the formation of a liquid intermediate and on product distribution during pyrolysis. Journal of Analitical and Applied Pyrolysis 100: 56-66.

Zheng, A.; L. Jiang; Z. Zhao; S. Chang; Z. Huang; K. Zhao; H. Li. 2016. Effect of hydrothermal treatment on chemical structure and pyrolysis behavior of eucalyptus wood. Energy and Fuels 30: 3057-3065.

Joko Sulistyo*, Ganis Lukmandaru, and Yunida Syafriani
Department of Forest Products Technology, Faculty of
Forestry, Universitas Gadjah Mada,
Jl. Agro No. 1, Bulaksumur, Yogyakarta, Indonesia
Tel. : +62-274-6491428
Fax. : +62-274-550541
*Email : jsulistyo@ugm.ac.id

Toshimitsu Hata
Laboratory of Innovative Humano-habitability, Research
Institute for Sustainable Humanosphere,
Kyoto University, Japan.

Sensho Honma
Hokaido Forestry Research Organization Forest Products
Research Institute, Asahikawa, Hokkaido, Japan

Improving the Physical Properties of Young Teak Wood through Phenol Formaldehyde Compregnation

Agung Dwi Saputra and Joko Sulistyo

Abstract

Young teak wood exhibits inferior properties due to a high proportion of juvenile wood and sapwood. The modification through compregnation of phenol formaldehyde is required to improve wood qualities. Therefore, this study aimed to observe the possibility of improving the physical properties of young teak wood (15 years) using phenol formaldehyde compregnation at various concentrations (5%, 10%, 15%) and pressing times (15, 30, 60 min). The results showed that phenol formaldehyde concentration produced retention with a maximum value of 31.19 kg/m^3. Based on wood without treatment (controls), the compregnation significantly increased the redness (a*) level by 45.57% and the specific gravity by 7.93%. The decreasing levels after treatment were observed in the brightness (L*) (by 36.56%), the yellowness (b*) (by 38.40%), and air-dried moisture contents by (by 5.44%). Furthermore, the reduction in hygroscopicity was observed in an equilibrium moisture content level in various relative humidity, as well as in increasing the stability dimension, though in a small magnitude.

Keywords: wood modification, pressure, higroscopicity, anisotropy, *Tectona grandis* L.f.

Introduction

The superior characteristics of teak wood include a good physical appearance and weathering resistance. However, young teak wood exhibits inferior properties due to the high content of sapwood and juvenile wood (Hidayati *et al.* 2015). Compared to mature wood, the juvenile has high proportion of early wood which causes lower density and strength. Furthermore, juvenile wood has high microfibril angles in the S2 layer of the cell wall. This form influences high longitudinal shrinkage and reduced transverse shrinkage, causing low dimensional stability (Shmulsky and Jones 2011).

Wood can be modified by physical and chemical methods or a combination of both. Wood modification is carried out through impregnation techniques using chemicals, heat densification, and pressure. There are several modification processes by impregnation based on various resin systems (Hill 2009). The modified wood products have a higher density than the original wood through a densification process where wood is impregnated with resin and compacted under pressure (compregnation). Phenol formaldehyde (PF) resins are commonly utilized in the wood industries as adhesives. Furthermore, phenol formaldehyde has several advantages in improving wood quality (Way *et al.* 2011; Ashaari *et al.*2015; Ang *et al.* 2014; Franke *et al.* 2017). Phenol formaldehyde resin impregnation and compression at high pressures significantly increase the strength of wood, especially flexural resistance, dimensional stability, and biological durability (Shams and Yano 2008; Nabil *et al.* 2016; Hartono *et al.* 2016). Therefore, this paper discussed on the improvement the physical properties of young teak wood by compregnation treatment using phenol formaldehyde.

Materials and Methods

Sample Preparation

The materials used in this study included three teak trees of 15 years old felled from Madiun Forest Management Unit, Perum Perhutani plantation. These trees were from thinning activities in which a total tree height of ± 6 m and diameter breast height of ± 13 cm. Sapwood samples were cut at the base part and sawn across the trunk with a length of approximately 1 m. Afterwards, the logs were sawn into boards in a flat sawn pattern. The boards were converted into specimens with a size of 2.5 × 2.5 × 20 cm for compregnation treatment and untreated (control). From these specimens, samples for moisture content (MC) and specific gravity (SG) (2 × 2 × 2 cm) as well as dimension stability (2 × 2 × 4 cm) were also taken according to British Standard (BSI 1957). Each sample was then coated with a flinkote paint on the cross-section of the wood to prevent compregnant substances from entering longitudinally. The test sample was then air-dried until it reached a MC of 12~15%. After the air-dry condition was achieved, the dimensions and initial weight of the sample were measured. The three individual trees were designed as replications.

Compregnation Process

The phenol formaldehyde (PA-302, PT. Pamolite Adhesive Industry, Probolinggo, Indonesia) was in liquid form with a solid resin content (RS) of 42% and molecular weight of 4000 Mn. The concentration of phenol formaldehyde solution (PF) was determined by the ratio of weight (w/w) of 5, 10, and 15%. Those levels were achieved by diluting PF resin with distilled water (formula $M_1V_1 = M_2V_2$). Furthermore, the compregnation process was preceded by air-drying the samples until 12~15% MC was reached. The initial weight was measured and the samples were then grouped according to the treatments. The test sample and PA solution were filled into the compregnator tank (Figure 1). The initial vacuum of 50-60 cmHg was applied for 15 min followed by pressing (10 kg/cm^2) for 15, 30, and 60 min. After the specified time was reached, the PF solution was removed and a final vacuum of 50-60 cmHg was applied for 15 min. The test sample was then air-dried and weighed.

Figure 1. Compregnation tank

Determination of Color Properties

Measurements were conducted using a spectrophotometer NF777 (Nipon Denshoku Co. Ind. Ltd., Japan). Air-dried woods were measured after compregnation three times for each sample at a different position. Three values were obtained including L* (brightness) with a scale of 0 (black) ~100 (white), a* (redness) with a (+) scale for red and (-) for green, and b* (yellow) with a (+) scale for yellow and (-) for blue.

Determination of Retention and Physical Properties

The retention was calculated from the dry weight of PF solution retained after treatment in a given volume of treated wood (kg/m^3). Measurements were carried out by weighing the wood after compregnation, minus the initial weight before. The MC was determined by oven method and SG by water displacement method (Marsoem *et al.* 2014). Furthermore, measurement of wood shrinkage was carried out in tangential, radial, and longitudinal directions from the condition of the wet MC to the oven-dried content. Anti-shrinkage efficiency (ASE) of each treatment variation was calculated using the following formula:

$$\text{ASE}\ (\%) = 100 \times [(Su - St)/Su] \quad \text{.........} \quad (1)$$

Where Su = volumetric shrinkage for untreated wood; St = volumetric shrinkage for treated wood.

Determination of Reduced Equilibrium Moisture Content

The test samples were measured for dimensions and weighed. Different relative humidities were achieved using saturated salt solutions (Young 1967). The test samples in three replications of each parameter were placed in a different desiccator on top of a cup containing ammonium sulfate, magnesium chloride, and potassium hydroxide to produce relative humidity (RH) of 81, 33, and 8% at a temperature of 25°C, respectively. The test samples were then weighed continuously until a constant weight was obtained. Afterwards, the test samples were dried at a temperature of 103 ± 2°C to determine the equilibrium moisture content (EMC). The percentage reduction in equilibrium moisture at saturation:

$$EMC_R\ (\%) = 100 \times [(EM_u - EMC_t)/EMC_u] \quad \text{.........} \quad (2)$$

Where EMC_R = reduction in equilibrium moisture content;
EMC_u = equilibrium moisture content for untreated wood;
EMC_t = equilibrium moisture content for treated wood.

Statistical Analysis

The effects of PF concentration and pressing time arranged in factorial design were calculated using analysis of variance (ANOVA) GLM procedures. The effects were taken into account only when significant at the 95% level using Type III Sums of Squares. Furthermore, the Tukey (Honestly Significant Difference) test was used to show further significant differences between groups. All statistics were performed using SPSS 12.0 software.

Results and Discussion

Retention Values

By ANOVA, it was observed that there was no significant interaction between the concentration and the pressing time factors (Table 1). The concentration factor affected all parameters except for longitudinal shrinkage and EMC at RH 33%. The pressing time factors had a significant effect only on retention and redness values. Retention is a measure of the concentration of preservative retained after treatment in a specified assay zone. The retention values obtained from the compregnation treatment using PF ranged from 13.47 to 31.19 kg/m^3 while the average highest value was obtained by a concentration of 15% and a pressing time of 30 minutes.

PF impregnation has been proven to increase the durability of the wood against termites or fungi attacks (Gascon-Garrod *et al.* 2015; Nabil *et al.* 2016). This experiment will be followed by bio-assay test to evaluate the PF resin act as a preservative in the next report. The retention value exceeded the minimum required for wood utilization for preservatives i.e. the equivalent of 5.30~15.89 kg/m^3 (Hunt and Garratt 1986). The increasing PF concentration and pressing time also caused an increase in the average retention amount (Figure 1). However, an increase in concentration of 10 to 15% and pressing time from 30 to 60 minutes did not show any significant differences. This is presumably due to the solution becoming saturated in the wood particularly in the lumen.

Table 1. The analysis of variance of of phenol formaldehyde concentration and pressing time effects

	Source of variation		
Properties	Concentration (A)	Pressing duration (B)	A x B
Retention	<0.01**	<0.01**	0.10
Specific gravity	0.01*	0.39	0.73
Air-dry moisture content	0.03*	0.01*	0.23
Longitudinal shrinkage	0.21	0.97	0.99
Radial shrinkage	0.04*	0.60	0.91
Tangential shrinkage	<0.01**	0.24	0.08
EMC–RH8–air-dry	<0.01**	0.49	0.86
EMC–RH8–wet	<0.01**	0.37	0.45
EMC–RH33–air-dry	0.40	0.73	0.74
EMC–RH33–wet	0.02*	0.17	0.41
EMC–RH81–air-dry	<0.01**	0.19	0.72
EMC–RH81–wet	<0.01**	0.68	0.43
Brightness (L*)	<0.01**	0.50	0.29
Redness (a*)	<0.01**	0.01*	0.51
Yellowness (b*)	<0.01**	0.56	0.43

Remark: SG = specific gravity; AD-MC = air-dry moisture content; RH = relative humidity; EMC = equilibrium moisture content

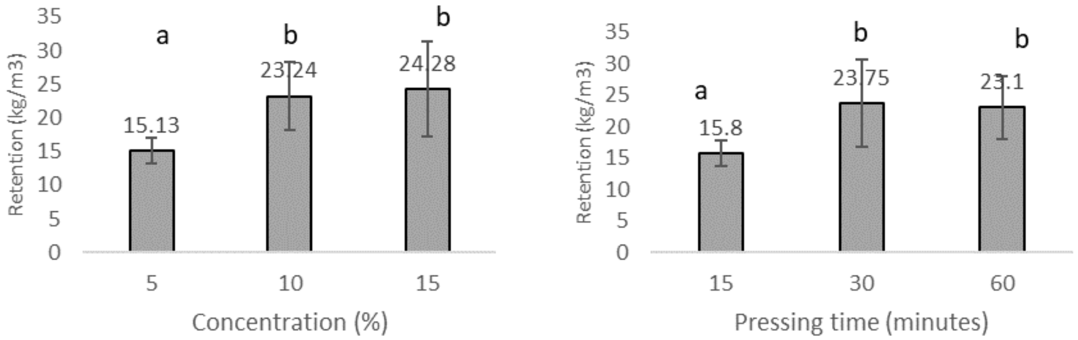

Figure 1. The effect of phenol formaldehyde concentration and pressing time on retention value. Mean of three trees, with the standard deviation error bar. The same letters are not statistically different at $P < 0.05$ by Tukey's test.

Color Properties

Color properties constituted supporting data to determine the effect of the compregnation treatment on young teak. Compregnation using PF caused the appearance of the wood to be darker, similar to the mature wood (Figure 2). The wood color was permanently changed and the solution thinly penetrated into the wood monitored by planing the surfaces. Unfortunately, the distance was not measured to obtain the actual penetration. Furthermore, increasing the concentration of PF up to 15% significantly decreased the values of L* (by 36.56%) and b* (by 38.40%) but increased the values of a* (by 45.57%) from the percentage of control values (Table 2).

PF resin gives red-brown color due to change in the pH of the wood/resin (Furuno *et al*. 2004; Kielmann *et al.* 2018) which is not occured for urea formaldehyde resin or poly-ethylene glycol treatment. The presence of PF had the same effect as extractives in heartwood where the greater the amount, the greater the color change. The increase in pressing time up to 30 min increased the a* value, signifying a more intensive reaction that resulted in the extractives in teak wood to have a reddish color. Teak extractives consisted quinone group with varying colors particulalrly in the heartwood part (Lukmandaru and Ogiyama 2005; Romagnoli *et al.* 2013). Therefore, further research is necessary to explore teak extractive compounds that experience color changes due to phenol formaldehyde impregnation in the sapwood part.

Figure 2. The appearance of teak wood control samples (brighter specimens) and after compregnation treatment (darker specimens) with phenol formaldehyde resin.

Table 2. The color properties of teak wood with compregnation treatment (phenol formaldehyde resin) (mean of three trees).

Concentration (%)	Pressing time (minutes)	L* (brightness)	a* (redness)	b* (yellowness)
5	15	45.2	12.5	14.6
	30	45.4	13.0	14.8
	60	46.6	13.0	13.7
10	15	41.5	13.7	11.9
	30	41.1	14.8	11.5
	60	39.9	15.1	11.7
15	15	34.2	14.6	9.8
	30	34.9	15.1	10.1
	60	32.2	14.9	10.0
Control		63.3	9.7	19.5

Specific Gravity and Moisture Content

The obtained wood SG of the study ranged from 0.61 to 0.68 (Table 3). Compared to the control (0.63), the highest improvement was achieved with a concentration of 10% and a pressing time of 15 min (0.68), although the increase in SG values only reached 7.93%. The impregnation PF in the parenchyma of the wood surface affected the SG increase (Sumardi *et al*. 1999). This relatively low value in this study indicates a few PF substances are able to penetrate into the cell wall structure. It is thought that the comparatively high initial density (0.63) of teak wood in this experiment partially affects the low penetreation rate. In earlier reports, the low initial specific gravity values in other species (0.5>) such as oil palm trunk (Sumardi *et al.* 1999; Aini *et al.* 1999; Hartono *et al.* 2016), sesenduk and jelutong (Adawiah *et al.* 2012; Ashaari *et al.* 2015) showed drastic increases in density levels. Another possibility is the unsuitable molecular weight of PF in this experiment (4000 Mn). PF (low molecular weight) with a concentration of 20% and hot pressing successfully increased wood density from 0.45 to 1.1 g/cm^3 in

Cryptomeria japonica wood (Shams *et al.* 2004). The effect of molecular weight of PF resin has been addressed by several researchers (Furuno *et al*. 2004; Rowell 2005; Aizat *et al.* 2017)

Wood is a hygroscopic material that adsorbs and desorbs water in liquid or vapor form from the atmosphere. The higher is the temperature or the lower the RH of the air, the lower is the EMC and vice versa. It is expected that the modified wood had a lower air-dried MC when compared to the control. It is also assumed that the decrease in MC was due to the presence of PF as a bulking agent that filled the wood cells. The air-dried MC of the treatment produced a range of 14.24~17.23% (Table 3). The lowest value was observed in the compregnation with a concentration of 5% and a pressing time of 15 minutes (14.24%) or a decrease of only 5.44% of the control value (15.60%).

Tabel 3. The specific gravity and moisture content of teak wood with compregnation treatment (phenol formaldehyde resin) (mean of three trees).

Concentration (%)	Pressing time (minutes)	SG	AD-MC (%)	Equilibrium moisture content (%)					
				RH8%-AD	RH8%-Wet	RH33%-AD	RH33%-Wet	RH81%-AD	RH81%-Wet
5	15	0.61	14.24	6.50	6.51	10.44	10.50	22.40	27.65
	30	0.61	14.60	6.46	6.64	10.24	10.75	22.25	26.31
	60	0.62	15.80	6.43	6.61	10.27	10.80	23.78	28.44
10	15	0.68	14.89	6.53	6.80	10.29	10.75	25.31	29.92
	30	0.63	17.23	6.64	6.74	10.62	11.06	28.02	30.73
	60	0.65	16.20	6.54	6.69	10.40	10.88	27.65	32.00
15	15	0.67	15.80	6.29	6.47	10.27	10.66	26.09	28.62
	30	0.65	16.13	6.23	6.53	10.28	10.68	28.11	30.60
	60	0.64	15.73	6.09	6.34	10.09	10.49	27.14	28.46
Control		0.63	15.60	6.33	6.51	10.30	10.80	24.11	30.21

Remark: SG = specific gravity; AD-MC = air-dry moisture content; RH = relative humidity.

At 8% and 33% RH, wood conditioned at the initial air-dried MC did not experience the mechanism of water adsorption from the surrounding environment (adsorption). On the other hand, the wood released water into the air (desorption) until it reached a state of equilibrium. For wood conditioned at different RH, a 5% concentration also showed the highest decrease in EMC at 81% RH (7.71~12.90%) but less significant at 8 and 33% RH. Furthermore, the addition of more than 5% concentration produced a higher EMC level than the control wood. The same result was also observed by Sumardi *et al.* (1999) and Aini *et al.* (1999) in oil palm wood. It is probable that in the wood treated initially with air-dried MC, some of the hygroscopic properties were reduced due to the previous drying process or hysteresis. Technically, resins are deposited in the wood cell walls extensively to reduce swelling on water immersion (Furuno *et al.* 2004). The ineffectiveness of PF in reducing the hygroscopicity of wood is assumed to be due to the few amount of PF that penetrated the cell wall, although it showed a high retention level. This is represented by the relatively small increase in SG values.

Dimensional Stability

The shrinkage parameters observed in this study included three main fiber directions of wood, i.e. longitudinal, radial, and tangential, as well as the value of ASE. The value of wood shrinkage observed was from wet to oven-dried conditions. Furthermore, the concentration factor significantly influenced the wood shrinkage in the radial and tangential directions. The compregnation treatment at a concentration of 5% showed a lower shrinkage value than the control wood and was more effective than other higher concentrations. This longitudinal shrinkage value obtained was in the range of 0.33~0.64%. A comparatively high value indicates the presence of juvenile wood (Shmulsky and Jones 2011). PF compregnation produced a lower shrinkage value than the control, with a percentage decrease of 11.86%; 3.73%; and 7.87% in the longitudinal; radial, and tangential directions, respectively.

The impregnation of phenol resin on wood increases its dimensional stability (Kollmann *et al.* 1975; Rowell 2005; Aizat *et al.* 2017). The penetration into the cell walls are the decisive factor for dimensional stability of the treated wood (Franke *et al.* 2017).This occurs through the penetration and enlargement of wood cell walls. The compregnation of PF reduced the shrinkage value of wood with the best treatment at a concentration of 5%. This agrees with previous studies on rubber wood (*Hevea brasiliensis* Muell Arg.) where compregnation with urea formaldehyde at a concentration of 5% produced the best effect on the physical and mechanical properties (Wedatama *et al.* 2014).

The effectiveness of the compregnation to stabilize wood dimensions was assessed through ASE values. Overall, it was observed that the highest ASE value was produced by a concentration factor of 5% alongside a pressing time of 15 min (43.85%). The lowest ASE value was produced by a concentration factor of 15% and a pressing time of 15 min. It is also noticed that the ASE values were less than 0% in several 10% concentration and 30-minute treatments as well as 15% concentration and 15- or 30-min treatments. For uncertain reason, it indicates those treatments caused less hydrophobic of the wood. The compregnation treatment was quite effective on the cross-section of the wood as evidenced by the higher ASE value in the longitudinal direction, compared to the radial and tangential. This is assumed to be due to the presence of large vessel cells for conducting the solution in a vertical direction. However, the value of anti-shrinkage efficiency (ASE) due to the PF compregnation treatment was still relatively low (50%>) to increase the dimensional stability of young teak wood. This is presumably because the type of PF used had a large molecular size to penetrate the cell wall. PF resin is deposited on the lumen surfaces (Hosseinpourpia *et al.* 2016). PF resin might bulk in cell wall while mostly the resin fill the lumen. Scanning electron microscope analysis will be helpful to confirm the inclusion of PF in the wood structure which causes different physical properties.

Tabel 4. The shrinkage and anti-shrink effficiency of teak wood with compregnation treatment (phenol formaldehyde resin) (mean of three trees).

Concentration (%)	Pressing time (minutes)	Shrinkage (%)			Anti-shrink effficiency (%)		
		Longitudinal	Radial	Tangential	Longitudinal	Radial	Tangential
5	15	0.33	2.67	4.04	43.85	17.25	36.42
	30	0.43	2.65	4.23	27.17	17.80	33.33
	60	0.34	2.62	5.22	42.89	18.54	17.87
10	15	0.54	3.17	5.63	8.71	1.66	11.31
	30	0.54	3.36	8.09	8.40	-4.20	-27.39
	60	0.61	3.10	6.25	-3.99	3.72	1.58
15	15	0.63	3.66	6.66	-7.62	-13.51	-4.88
	30	0.64	3.62	6.54	-8.93	-12.44	-3.05
	60	0.58	3.02	5.99	0.58	6.15	5.73
Control		0.59	3.22	6.35			

Conclusions

The physical properties of the teak sapwood had been improved by the PF treatment (concentration and pressing time). The maximum retention value was produced at a concentration of 10% and a pressing time of 30 min (31.19 kg/m^3) which exceeded the minimum required for wood utilization for preservatives. The increase in the SG value of the control reached 7.93% by a concentration of 10% and a pressing time of 15 min (0.63 to 0.68). The compregnation treatment with a concentration of 5% produced the best results on hygroscopic properties and dimensional stability, although the decrease was not as high as expected, while the concentration of 15% caused a drastic change in color properties. Pressing time only affected significantly air-dried MC and redness (a*) values. Therefore, the compregnation of phenol formaldehyde in young teak wood with the lower molecular weight resin for maximizing penetration into the cell wall of the wood should be explored as a subsequent study.

References

Adawiah, M.A.R.; A. Zaidon; F.A.N. Izreen; E.S. Bakar; S.M.Hamami; M.T. Paridah. 2012. Addition of urea as formaldehyde scavenger for low molecular weight phenol formaldehyde-treated compreg wood. Journal of Tropical Forest Science 24(3): 348-357.

Aini, N.S.; Edi S.B.; I. Sumardi. 1999. Perbaikan kualitas kayu sawit dengan teknik impregnasi/ compregnasi (iii): Compregnasi kayu sawit dengan fenol formaldehida. Prosiding Seminar Nasional II Masyarakat Peneliti Kayu Indonesia. p. 369. Yogyakarta.

Aizat, G.; A. Zaidon; S.H. Lee; S.B. Ed; B. Paiman. 2017.A comparison between the properties of low and medium molecular weight phenol formaldehyde resin-treated laminated *compreg* oil palm wood. International Forestry Review 19(S3): 1-11.

Ang, A.F.; A. Zaidon; E.S. Bakar; M. Hamami; U.M.K. Anwar; M. Jawaid. 2014. Possibility of improving the properties of Mahang wood (*Macaranga* sp.) through phenolic c*ompreg* technique. Sains Malaysiana 43(3): 219-225.

Ashaari, Z.; S.H. Lee; M.N.Mustamel; N.F.M. Salleh. 2015. Strength improvement of jelutong (*Dyera costulata*) wood via phenolic resin treatments. Journal Indian Acadademy of Wood Science 12(2): 132-136.

British Standard Institution. 1957. British Standard Methods of Testing Small Clear Speciments of Timber. British Standard Institution, Royal Charter British Standard House. London.

Franke, T.; A. Mund; C. Lenz; N. Herold; A. Pfriem. 2017. Microscopic and macroscopic swelling and dimensional stability of beech wood impregnated with phenol-formaldehyde. Pro Ligno 13(4): 373-378.

Furuno, T.; Y. Imamura; H. Kajita. 2004. The modifcation of wood by treatment with low molecular weight phenol-formaldehyde resin: a properties enhancement with neutralized phenolic-resin and resin penetration into wood cell walls. Wood Science and Technology 37(5): 349-361.

Gascon-Garrido, P.; H. Militz; C.Mai, M.F. Thévenon. 2015. Enhanced termite resistance of Scots pine (*Pinus sylvestris* l.) Solid wood by phenol- formaldehyde treatment. Wood Research 60 (6): 873-880 .

Hartono, R.; W. Hidayat; I. Wahyudi; F. Febrianto; W. Dwianto; J.H. Jang; N.H. Kim. 2016. Effect of phenol formaldehyde impregnation on the physical and mechanical properties of soft-inner part of oil palm trunk. Journal of Korean Wood Science and Technology 44(6): 842-851.

Hidayati, F.; J. Sulistyo; G. Lukmandaru; T. Listyanto; H. Praptoyo; R. Pujiarti. 2015. Physical and mechanical properties of 10-Year old superior and conventional teak planted in Randublatung Central Java Indonesia.. Jurnal Ilmu Teknologi Kayu Tropis 13(1): 11-21.

Hill, C.A.S. 2009. The potential for the use of modified wood products in the built environment. Proceedings of The 11th International Conference on Non-conventional Materials and Technologies. p1-6. Bath, UK.

Hosseinpourpia, R.; S. Adamopoulos; C. Mai. 2016. Dynamic vapour sorption of wood and holocellulose modifed with thermosetting resins. Wood Science and Technology 50(1): 165-178.

Hunt, GM.; G.A. Garratt. 1986. Pengawetan Kayu. 1st Edition. Terjemahan M. Yusuf. Akademika Pressindo. Jakarta.

Kielmann, B.C.; K. Butter; C. Mai. 2018. Modifcation of wood with formulations of phenolic resin and iron-tannin-complexes to improve material properties and expand colour variety. European Journal of Wood Product 76: 259-267.

Kollmann, F.P.F.; E.W. Kuenzi, A.J. Stamm. 1975. Principles of Wood Science and Technology. Springer-Verlag Berlin Heidelberg. New York.

Lukmandaru, G; K. Ogiyama 2005. Bioactive compounds from ethyl acetate extract of teakwood (*Tectona grandis* L.f.). Proceedings of the 6th International Wood Science Symposium LIPI-JSPS Core, pp 346-350, Bali.

Marsoem, S.N.; V.E.Prasetyo; J. Sulistyo; Sudaryono; G. Lukmandaru. 2014. Studi mutu kayu jati di hutan rakyat Gunungkidul. III. Sifat fisika kayu. Jurnal Ilmu Kehutanan 8(2): 75-88.

Nabil, F.L.; A. Zaidon; U.K.M. Anwar; E.S. Bakar; S.H. Lee; M.T. Paridah. 2016. Impregnation of sesenduk (*Endospermum diadenum*) wood with phenol formaldehyde and nanoclay admixture: Effect on fungal decay and termites attack. Sains Malaysiana 45(2): 255-262.

Romagnoli M.; E. Segoloni; M. Luna; A. Margaritelli; M. Gatti; U. Santamaria; V. Vinciguerra. 2013. Wood colour in lapacho (*Tabebuia serratifolia*): Chemical composition and industrial implications. Wood Science and Technology 47: 701-716.

Rowell, R.M.. 2005. Chemical Modification of Wood. In: Handbook of Wood Chemistry, Wood Composites, Rowell R.M. (Ed.). CRC Press, Boco Raton, pp: 381-420.

Shams, M.I.; H. Yano, K. Endou. 2004. Compressive deformation of wood impregnated with low molecular weight phenol formaldehyde (PF) resin I: Effects of pressing pressure and pressure holding. Journal Wood Science 50: 337-342.

Shams, M.I.; H. Yano. 2008. A new method for obtaining high strength phenol formaldehyde resin-impregnated wood composites at low pressing pressure. Journal of Tropical Forest Science 21(2): 175-180.

Shmulsky. R.; P.D. Jones. 2011. Forest Products and Wood Science: An Introduction, Sixth Edition. John Wiley & Sons, Inc.

Sumardi, I., Edi, S.B. dan Y.S. Hadi. 1999. Perbaikan kualitas kayu sawit dengan teknik impregnasi/ compregnasi (II) : Impregnasi kayu sawit dengan fenol formaldehida. Prosiding Seminar Nasional II Masyarakat Peneliti Kayu Indonesia. pp 360-368. Yogyakarta.

Young, J.F. 1967. Humidity control in the laboratory using salt solutions - A review. Journal of Applied Chemistry 17: 241-245.

Way, C.Y; E.S. Bakar; Z. Ashaari; M.H. Sahri. 2011. Treatment of oil palm wood with low-molecular weight phenol formaldehyde resin and its planing characteristics. Wood Research Journal 1(1): 7-12.

Wedatama, S.; JPG Sutapa; D. Irawati. 2014. Peningkatan kualitas kayu karet dengan compregnasi menggunakan urea formaldehida. Prosiding Seminar Nasional Masyarakat Peneliti Kayu Indonesia (MAPEKI) XVI. 113-116.

Agung Dwi Saputra and Joko Sulistyo*,
Dept. of Forest Products Technology, Faculty of Forestry,
Universitas Gadjah Mada,
Jl. Agro No. 1, Bulaksumur, Yogyakarta, Indonesia
Tel. : +62-274-6491428
Fax. : +62-274-550541
*Email : jsulistyo@ugm.ac.id

The Role of Canopy Structure of *Terminalia catappa* Linn. on Decreasing Light Penetration and Ambient Temperature as Climate Change Mitigation

Marjenah, Karyati, Sri Sarminah, Muhammad Syafrudin, Irwan,
Anjas Aswar, and Indar Ruardianto

Abstract

Tropical almond (*Terminalia catappa* Linn.) is a tree that usually grows on the seashore which has a shady canopy. This tree is usually planted as an ornamental plant or a shade plant on the side of the road. The presence of the *Terminalia catappa* tree can provide coolness if the tree is planted in the garden or in the yard or along the roadside. This research was carried out in East Kalimantan which the sampling location were Balikpapan, Samarinda and Tenggarong City. Twenty-five trees of tropical almond were set in each city which were used as the tested samples trees. Data taken includes a) data on physical environmental characteristics (light intensity, ambient temperature and humidity) which performed under the canopy and outside canopy on each tree sample, and b) data on morphological characteristics (location, height, diameter at breast height, and shape / width of crown). The result showed that there was relationship between the volume of the tropical almond tree canopy on light penetration under and outside canopy of the tropical almond tree which indicated that there was an effect of the volume of the tropical almond tree canopy on light penetration. The light penetration will decrease along with the increase of canopy volume. There were relationships among light penetration and ambient temperature as well as relative humidity under and outside canopy of the tropical almond tree which indicated that there were the effect of light penetration on a decrease in ambient temperature and increase in relative humidity. The tropical almond tree can be used as a roadside shade tree as well as an ornamental plants in gardens or in the yard, because it can lower the ambient temperature and provide coolness.

Keywords: Shade tree, Tropical almond, translucence, ambient temperature, reduce disaster risk.

Introduction

Terminalia catappa Linn. (Tropical almond) is the name of a kind of shade tree that usually grows by the beach (Thomson and Evans 2006). Rapid growth, forming a beautiful tiers of storied, so Tropical almond often used as shade trees in the parks and roadside. Tropical almond is a deciduous trees. In East Kalimantan, Tropical almond shedding out its leaves twice a year, the first is on January to March and the second is on July to September. The grow of new shoots (vegetative) is usually followed by the emergence of generative shoots. Tropical almond leaves before shedding change its color first; from green, yellow-orange, then brown-red to purple and then fall. At the time Tropical almond leaves orange, red-purple will give the beauty as it was autumn (Marjenah and Putri 2017a). In India, Raju *et al*. (2012) recorded information that *T. catappa* changes foliage twice in a year, the first during February-March and the second during June-August, each time with the shedding leaves and a new foliage puts forth.

T. catappa, widely called Indian almond or Tropical almond, has a number of other local names where English is spoken: Barbados almond, Bastard almond, Bengal almond, Country almond, Demarara almond, False kamani, Fijian almond, Malabar almond, Malay almond, Sea almond, Singapore almond, Story tree, Tavola nut, and West Indian almond. It is known as alconorque in Nicoya, Costa Rica; almendrillo, almendro, almendro de la India, or almendron (generally in Spanish-speaking areas); almendro del pais (in El Salvador); amandelboom (Surinam); amandier de Cayenne (French Guiana); amandier des indies (Haiti); amandier des tropiques (Gabon); amendoeira (Brazil); badam (India); badamier (southeast Asia and West Africa); castafia (Peru); castafiola, chapeu de sol, and guarda-sol (Brazil); kalumpit (Philippines); kamani-haole (Hawaii); ketapang (Malaysia); kotamba (Colombia); parasol (Brazil); saori (Solomon Islands); talie (Samoa); talisai (Philippines); tavola (Fiji); tipapop and tipop (Ponape, Caroline Islands); tivi (Fiji); white bombway (Andaman Islands); wilde amandel (Netherlands Antilles); zanmande (Haiti). There are many other names in the dialects of the Far East (Morton 1985).

T. catappa is also usually planted in various places because it provides shade and the leaves can filter out a lot of sunlight. There are several sidewalk garden areas that are suitable for tropical almond trees, such as school sidewalks, office buildings because they usually have a large enough space. The benefits of planting tropical almond trees in the school garden or office area will have an impact on the environment that feels more shady, because the amount of sunlight is filtered by the leaves and twigs, thus allowing the area to be cool and increase concentration power.

Presenting *T. catappa* tree in the yard can make it fresher and cooler because it can block the hot sun in the yard. This *T. catappa* tree can grow to tens of meters and a branch span of up to 4 meters or more. A wide stretch of branches / twigs will cause shade under the *T. catappa* tree, in addition to reducing the intensity of light reaching the ground, this can also lower the air temperature.

Structure of the canopy of trees can be understood as the appearance of whole branches, twigs, and leaves. The density of the tree canopy relates to the optimal intensity of sunlight, which is divided into three criteria: mild (rare), medium and heavy. This criterion is based on the high intensity of the sun that is able to penetrate the underlying strata of plants (Sutisna 2001 in Rotinsulu and Susilowaty 2014).

Light is considered the most limiting resource for trees in tropical rainforest biomes, with light penetration in the vertical dimension of rainforests declining markedly with increasing canopy depth (Weerasinghe *et al*. 2014). As a result, within a closed canopy, the availability of light can be reduced by up to 50-fold from the top of canopy compared with foliage in the shaded understory (Baldocchi *et al.* 2002).

Mitigation is an effort to reduce the greenhouse effect so that it can slow down the rate of global warming. The United Nations defines climate change mitigation as human intervention in reducing sources of greenhouse gas (GHG) emissions, especially those related to human production and consumption activities. Climate change mitigation is an effort to control climate change through activities that can reduce emissions or allow the absorption of greenhouse gases from various emission sources (Perpres RI No 46/2008).

Climate and its elements are important things to be considered and studied as well as possible, because their influence often creates big problems for humans, as well as other living things. This problem is a challenge for humans where he must try to overcome it by avoiding or minimizing the effects that do not benefit human life.

Climate tends to change by human activities such as urbanization, industrialization, deforestation, and by natural activities such as continental shifts, volcanic eruptions, change in earth's orbit to the sun, sun stains, and El Nino event. Environmental development needs to pay attention to efforts to maintain natural systems and need to analyze the impact of development on the climate.

The ambient temperature in the forest is greatly influenced by the intensity of sunlight entering the soil surface. If the canopy is getting thicker, the temperature in the forest will decrease, if the canopy is not too dense, the intensity of the incoming sunlight will increase and the ambient temperature at the ground surface will also increase (Utomo 2006).

The purpose of the research was to find out the ability of tropical almond canopy in lowering light penetration and ambient temperature; relationship of canopy volume to light intensity, light penetration and ambient temperature as well as relative humidity.

Material and Methods

Study Area

Seventy-five trees of *T. catappa* were randomly selected from three locations in East Kalimantan Province, namely Balikpapan, Samarinda, and Tenggarong City. *T. catappa* trees are selected as research objects that grow solitary planted on the roadside as shade plants. The research was conducted in January-October 2019.

Collection and Preparation of Samples

The sampling stages are as follows: (i) Measuring *T. catappa* tree and selecting the tree which has minimum diameter of 10 cm at a height of 1.3 m from the ground as a sample; (ii) Measuring the width of the crown/canopy (Figure 1) which covers projections according to each of the four main points to the compass (North, South, East, and West).

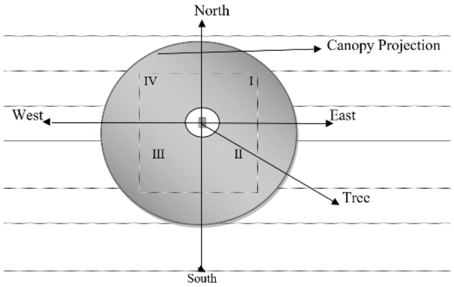

Figure 1. Projection of Canopy and Quadrant for Extending the Canopy Area (Marjenah and Putri 2017b)

Physical Environmental Characteristics

Observations or measurements of ambient temperature and humidity in the field, under canopy and open area were done once in each sample tree by using thermo-hygrometer. Measurement of light intensity is performed on every tree sample using light meter. Measurement of climate elements was repeated three times.

Data Analysis

Data analysed were using regression analysis to determine the relationship between the independent variable and the dependent variable.

Result and Discussion

The canopy thickness of Tropical almond is predicted to reduce the intensity of light that penetrates the canopy, furthermore canopy thickness can reduce ambient temperature. The presence of Tropical almond planted on the roadside as ornamental plants can reduce the temperature of the urban environment. In simple terms, it can be stated that the role of the canopy of the Tropical the roadside as ornamental plants can reduce the temperature of the urban environment. In simple terms, it can be stated that the role of the canopy of the Tropical almond in mitigating climate change is to reduce the temperature.

Relationship of canopy structure and climate elements (light Intensity, air temperature, and air humidity) is shown in the Figure 2, 3, and 4.

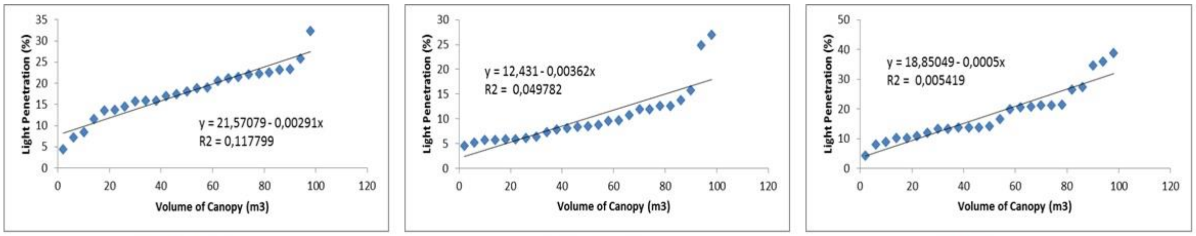

(a) Balikpapan

(b) Samarinda

(c) Tenggarong

Figure 2. Relationship Between Canopy Structure and Light Penetration in the Cities of Balikpapan, Samarinda and Tenggarong

Canopy Structure and Light Intensity

The results show that there was relationship between the volume of the tropical almond tree canopy on light penetration under and outside of canopy of the tropical almond tree which indicated that there was an effect of the volume of the tropical almond tree canopy on light penetration. Figure 2 show several linear regressions that tend to decrease. The constant value (b) appears to have decreased in the cities of Balikpapan, Samarinda and Tenggarong. This indicated that there was a negative relationship. If there is an increase in the volume of the canopy, there will be a decrease in light penetration. R square amounting 0.1178; 0.0498 and 0.0054 for the cities of Balikpapan, Samarinda and Tenggarong, respectively, this indicates a very weak relationship between canopy volume and light penetration. 11.78%; 4.98% and 0.54% light penetration is affected by the volume of the canopy. The rest is influenced by other factors.

Light is considered the most limiting resource for trees in tropical rainforest biomes, with light penetration in the vertical dimension of rainforests declining markedly with increasing canopy depth. As a result, within a closed canopy, the availability of light can be reduced by up 50-fold from the top of canopy compared with foliage in the shaded understory (Baldocchi *et al*. 2002). In terms of usage and space requirements grow, the width of the canopy has an important role. Canopy width can be used to predict light intensity that is exposed to trees and which is obstructed and intercepted in the canopy of a stand (Fu *et al*. 2013).

Light penetration into the canopy is affected by the volume of the canopy. The thicker of the canopy, more and more difficult it is for the light to penetrate. The thickness of the crown is influenced by the density of the leaves and the size of the leaves. Tropical almond leaves are generally large and absorb more light. In addition, the penetration of light into the canopy is also influenced by the direction of the light and the angle of the leaves. Leaf area is the morphological characteristics commonly used to determine the development of the canopy. Leaf canopy structure, especially of leaf angle, is relative to vertical line. Plants with horizontal leaves proceed 30-40% of the light coming through each unit of index of leaf area, while the upright leaves can proceed 45-65% of the light. With leaves that are perpendicular to sunlight on bright sunlight, the growth rate of the crop will be theoretically enhanced by the spreading of the more evenly distributed light in the canopy with upright leaves (Goldsworthy and Fisher 1992).

The influence of plant canopy on microclimate is directly and indirectly related to the attendent of canopy and stem. Branches and leaves reflect and absorb some of the sun's radiation during the day, allowing less energy to reach the ground under the canopy (Arx *et al*. 2012).

Light is considered the most limiting resource for trees in tropical rainforest biomes, with light penetration in the vertical dimension of rainforests declining markedly with increasing canopy depth. As a result, within a closed canopy, the availability of light can be reduced by up 50-fold from the top of canopy compared with foliage in the shaded understory (Baldocchi *et al*. 2002). In terms of usage and space requirements grow, the width of the canopy has an important role. Canopy width can be used to predict light intensity that is exposed to trees and which is obstructed and intercepted in the canopy of a stand (Fu *et al*. 2013).

Light penetration into the canopy to the ground (forest floor) affects the ambient temperature and humidity conditions. The light that penetrates the canopy affects the temperature. when the light penetration is high, the air temperature will be high as well. Meanwhile, temperature affects the humidity of the air, when the temperature is high the humidity will be low. Air humidity is inversely proportional to temperature.

Spatial and temporal variations in canopy structure and function affect the microclimate of the canopy, and consequently, affect temperature and humidity in various ways. For example, interactions between structural and functional properties of forests alter turbulence within and over the canopy, light penetration, heat load on leaves and soil, and physiological resistance to water and air.

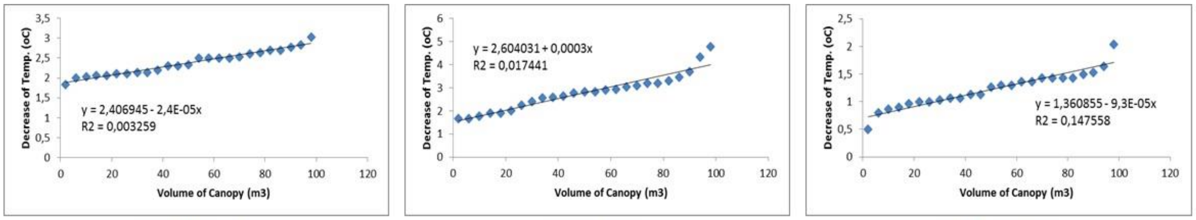

(a) Balikpapan (b) Samarinda (c) Tenggarong

Figure 3. Relationship Between Canopy Structure and Decreased of Ambient Temperature in the Cities of Balikpapan, Samarinda and Tenggarong

Canopy Structure and Air Temperature

The temperature difference that occurs between the outside and under canopy is not only caused by the canopy structure which causes less light penetration from the top of the canopy to the bottom of the canopy, more than that it is also caused by the transpiration of leaves from the tree crown which causes coolness in the canopy and under the canopy.The decrease in ambient temperature is the difference between the temperature under canopy and outside canopy. Light penetration into the canopy has an effect on the light intensity reaching the ground which in turn will also affect the temperature below the canopy.

The results of the study stated that linear regression of the relationship between canopy structure and decreased ambient temperature of tropical almond tree and outside canopy indicated that there was an effect of light penetration of the tropical almond canopy on a decrease in ambient temperature. Figure 3 shows a linear regression that tends to increase. The value of the constant (b) appears to have increased in the cities of Balikpapan, Samarinda and Tenggarong. The thickness of the canopy will obstruct light penetration and will further lower the ambient temperature.

R square 0.0033; 0.0174 and 0.1476 for the cities of Balikpapan, Samarinda and Tenggarong, respectively, this indicates a very weak relationship between light penetration and decreased of ambient temperature. 0.33%; 1.74% and 14.76% decrease in ambient temperature in those cities are affected by light penetration in the canopy. The rest is influenced by other factors.

The air temperature on the earth's surface is relative, depending on the factors that influence it, such as the length of the sun's exposure, the tilt of the sun, cloud conditions, and the condition of the earth's surface. Air temperature varies with place and from time to time on the earth's surface. According to the place the air temperature varies vertically and horizontally and according to time from hour to hour in the day, and according to the month of the year (Satwiko 2009).

Canopy Structure and Relative Humidity

The relative humidity under the canopy is influenced by the air temperature. Humidity and temperature are two related parameters, when the air temperature is low, the relative humidity tends to be high and vice versa. If the air temperature is higher, the relative humidity will be lower. Vice versa, the lower the air temperature, the air humidity will be higher.

The results of the study stated that linear regression indicated that there was an effect of canopy structure of the tropical almond canopy on an increase in relative humidity. Figure 4 shows a linear regression that tends to increase. The value of the constant (b) appears to have increased in the cities of Balikpapan, Samarinda and Tenggarong. This indicates that there is a positive relationship.

R square 0.00865; 0.0217 and 0.0547 for the cities of Balikpapan, Samarinda and Tenggarong, respectively, this indicates a very weak relationship between light penetration and humidity. 0.865%; 2.17% and 5.47% humidity are affected by canopy structure. The rest is influenced by other factors.

High light environments, particularly those with other stresses such as drought and high temperatures, impose very different demands on canopy structure than those imposed in the understory. Under full sunlight conditions, there is strong evidence for the fundamental role that canopy structure plays as the first line of defense against temperature extremes and photoinhibition through avoidance of excessive radiation loads on the leaf surfaces (Pearcy *et al.* 2005).

Canopy layer is determined by the balance between the biochemically and physiologically limited demand of leaves and the diffusion-limited supply from the atmosphere and through the leaf boundary layer (Sinoquet, *et al.* 2001). The quantity of the light in natural environments can vary over several orders of magnitude and on a time scale that ranges from seconds to seasons. Because light is such an important environmental parameter, plants have evolved numerous biochemical and developmental responses to light that help to optimize photosynthesis and growth (Muller *et al.* 2001). The realism of which a canopy and its pattern of growth can be reconstructed is quite remarkable.

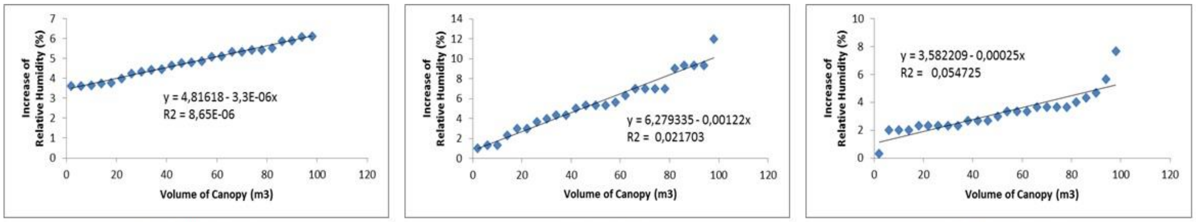

(a) Balikpapan (b) Samarinda (c) Tenggarong

Figure 4. Relationship Between Canopy Structure and Increased of Relative Humidity in the Cities of Balikpapan, Samarinda and Tenggarong

Although there is no inherent limitation to doing so, developmental-rule-based models have not been used much to evaluate the functional role canopy structure on the physiological or ecological performance of plants (Pearcy *et al*. 2005). At the canopy scale, biophysical models vary in the way they represent canopy structure and function. Increased accuracy achieved by using multiple source abstractions, a concept that explains the different environment and sunlight as well as shaded leaves.

Conclusions

Light penetration by canopy tropical almonds can lower the ambient temperature. The lower ambient temperature will cause the relative humidity to increase. then it will make the area around the tropical almond tree cooler.

Acknowledgements

We would like to express our gratitude to Riyayatsyah, Ibnu Suyuti, Rizky Dirga, and Muhammad Said, for their assistance in the field. Many thanks to the members of Silviculture Laboratory, Faculty of Forestry, Mulawarman University, Samarinda, Indonesia for supporting this project.

References

Arx GV, Dobbertin M, Rebetez M. 2012. Spatio-temporal effects of forest canopy on understory microclimate in along-term experiment in Switzerland. Agric For Meteor 166-167 (2012): 144-155.

Baldocchi, D.D. , K.B. Wilson., and L.H. Gu. 2002. How The Environment, Canopy Structure And Canopy Physiological Functioning Influence Carbon, Water And Energy Fluxes Of A Temperate Broad-Leaved Deciduous Forest—An Assessment With The Biophysical Model CANOAK. Tree Physiology 22, 1065-1077. *Heron Publishing—Victoria, Canada*

Fu, L., H Sun, R.P Sharma, Y Lei, H Zhang, and S Tan. 2013. Nonlinear Mixed- effects Crown Width Models for individual trees of Chinese fir (*Cunninghamia lanceolata*) in South-Central China. Forest Ecology and Management. 302: 210-220.

Goldsworthy PR, Fisher NM. 1992. The Physiology of Tropical Field Crops. (In Bahasa Indonesia. Translator: Tohari). Gadjah Mada University Press. Yogyakarta.

Marjenah and N.P. Putri. 2017a. Morphological Characteristic and Physical Environment of *Terminalia catappa* in East Kalimantan, Indonesia. Asia Journal of Forestry. Volume 1, Number 1, June 2017. Pages: 33-39.
DOI: 10.13057/asianjfor/r010105

Marjenah and N.P. Putri. 2017b. Pengaruh Elevasi Terhadap Produksi Buah Ketapang (*Terminalia catappa* Linn.) Sebagai Bahan Baku Pembuatan Biodiesel. Jurnal HutanTropis. 5(3): 244-251.

Morton, J.F. 1985. Indian Almond *(Terminalia catappa*), Salt-tolerant, Useful, Tropical Tree with “Nut” Worthy of Improvement. Economic Botany, 39(2). Pp. 101-112. The New York Botanical Garden.

Muller, P., X. P. Li., and K. K. Niyogi. 2001. Non-Photochemical. A Response to Excess Light Energy. Department of Plant and Microbial Biology, University of California, Berkeley, California 94720–3102. *Plant Physiology* Vol. 125, 2001.

Pearcy, R. W. , H. Muraoka., and F. Valladares. 2005. Crown Architecture In Sun And Shade Environments: Assessing Function And Trade-Offs With A Three-Dimensional Simulation Model. *New Phytologist* (2005) **166**: 791-800.

Perpres RI No 46/2008 Tentang Dewan Nasional Perubahan Iklim.

Raju AJS, Lakshmi PV, Ramana KV. 2012. Reproductive ecology of *Terminalia pallida* Brandis (Combretaceae), an endemic and medicinal tree species of India. Curr Sci 102 (6): -.

Rotinsulu, J.M. and Susilowaty. 2014. Pengaruh Bentuk Tajuk Pohon Terhadap Faktor Lingkungan dan Pertumbuhan Rotan pada Sistem Agroforestri. Prosiding Seminar Nasional Silvikultur Ke IV. 250-262.

Satwiko, P. 2009. Fisika Bangunan. Yogyakarta: Penerbit Andi

Sinoquet, H., L.X Roux, B. Adam, T. Ameglio, F.A. Daudet. 2001. RATP: a model for simulating the spatial distribution of radiation absorption, transpiration and photosynthesis within canopies: application to an isolated tree crown. Plant, Cell and Environment (2001) 24, 395-406.

Thomson LAJ, and Evans B. 2006. *Terminalia catappa*. Species Profiles for Pacific Island Agroforestry. www.traditionaltree.org.

Utomo, B. 2006. Hutan Sebagai Masyarakat Tumbuhan Hubungannya dengan Lingkungan. Library.usu.ac.id.

Weerasinghe, L. K., D. Creek., K. Y. Crous, S. Xiang, M. J. Liddell, Matthew H. Turnbull and O. K. Atkin. 2014. Canopy Position Affects The Relationships Between Leaf Respiration And Associated Traits In A Tropical Rainforest In Far North Queensland. Tree Physiology Online at http://www.treephys.oxfordjournals.org Published by Oxford University Press. Tree Physiology Volume 34, 2014.

Marjenah, Karyati, Sri Sarminah, Muhammad Syafrudin, Irwan, Anjas Aswar, and Indar Ruardianto
Silviculture Laboratory, Faculty of Forestry,
University of Mulawarman
Kampus Gunung Kelua. Jl. Penajam P.O. Box 1013
Samarinda 75116, East Kalimantan, Indonesia.
Tel. : +62-541-735 089, 749 068;
Fax. : +62-541-735 379
E-mail : marjenah-umar@yahoo.com

Volume 12, Number 1, April 2021 ISSN 2087-3840; e-ISSN 2774-9320

WOOD RESEARCH Journal

Journal of Indonesian Wood Research Society

Annals of the Wood Research Journal

Wood Research Journal is the official journal of the Indonesian Wood Research Society. This journal is an international medium in exchanging, sharing and discussing the science and technology of wood.

Aims and Scope

The journal publishes original manuscripts of basic and applied research of wood science and technology related to Anatomy, Properties, Quality Enhancement, Machining, Engineering and Constructions, Panel and Composites, Entomology and Preservation, Chemistry, Non Wood Forest Products, Pulp and Papers, Biomass Energy, and Biotechnology. Besides that, this journal also publishes review manuscripts which topics are decided by the Editors.

Imprint

WRJ is published by Indonesian Wood Research Society
ISSN print: 2087-3840
Electronic edition is available at:
http://ejournalmapeki.org/index.php/wrj

Publication Frequency

Journal is published in one volume of two issues per year (April and October).

Peer Review Policy

WRJ reviewing policies are: Every submitted paper will be reviewed by at least two peer reviewers. Reviewing process will consider novelty, objectivity, method, scientific impact, conclusion and references.

General Remarks

Manuscripts will be accepted for publications are those discussing and containing results of research on wood science and technology, and reviews on specific topics, which are decided by the Editors and have not been published elsewhere. Authors are requested to correct the manuscripts accepted for publications as suggested by the Reviewers. Editors could change positions of Figures and Tables.

Manuscripts Preparations

1. Manuscripts must be in English, typewritten using Word, Arial Narrow, single space, 3 cm of left and right margin and 2.5 cm of top and bottom margin of a Letter paper size. Title is printed with a font size of 14 pt, Authors are of 12 pt, and Text is of 10 pt.
2. Manuscripts should be checked for spelling and grammar by a native speaker.
3. Manuscripts compositions:

3.1. Title
3.2. Complete name of Authors
3.3. Abstract
3.4. Key words
3.5. Texts:
Introduction
Materials and Methods Results and Discussion
Conclusions (and Suggestions) References
Name and complete address of Authors
Appendix
4.Other rules:
4.1. Names of wood are followed by Botanical Name.
4.2. Values between are written using this symbol (~), e.g. 3.75 ~ 8.92%.
4.3. Editors could modify Figures without changing their substantial meaning.
4.4. References are arranged from A to Z.
4.5. References in text are written as this example: (Palomar *et al.* 1990; Arancon 1997).
4.6. Examples of writing of References: Altschul, S.F.; T.L. Madden; A.A. Schäffer; J. Zhang; Z. Zhang; W. Miller; D.J. Lipman. 1997. Gapped BLAST and PSI-BLAST: A New Generation of Protein Database Search Programs. Nucleic Acids Res. 25: 3389-3402.

Editorial Address

Research Center for Biomaterials, Indonesian Institute of Sciences
Jl. Raya Bogor Km 46, Cibinong, Bogor 16911, Indonesia
Tel/Fax : +62-21-87914511/87914510
E-mail : ejournal.wrj@gmail.com
Web-site : www.ejournalmapeki.org

Volume 12, Number 1, April 2021 ISSN 2087-3840; e-ISSN 2774-9320

WOOD RESEARCH Journal

Journal of Indonesian Wood Research Society

Example of Table and Figure

Table 1. Effects of temperature on *in vitro* growth of seedlings.

Temp. (°C)	Shoot length (mm)	Number of leaf	Fresh weight (g)
25	59.2 ± 10.6^{c}	4.5 ± 0.8^{a}	0.29 ± 0.13^{a}
27	88.5 ± 9.3^{a}	4.8 ± 0.9^{a}	0.40 ± 0.12^{a}
29	75.0 ± 11.1^{b}	3.8 ± 0.6^{a}	0.30 ± 0.07^{a}

Note: Values (average ± standard deviation) with different letters are statistically significant according to Tukey's multiple comparison test. Data were recorded after 4 weeks of culture. MS medium was used as a basal medium without any PGRs. Number of sample = 10.

Source: Chujo *et al.* 2010.

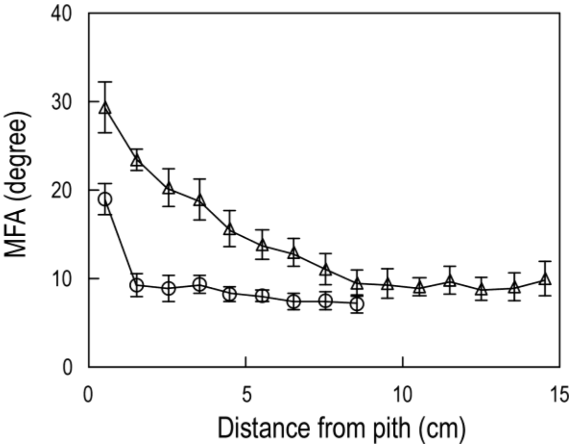

Figure 3. Radial variation of microfibril angle of the S2 layer in tracheid. Open circle, *Agathis* sp.; open triangle, *Pinus insularis*; Bars indicate the standard deviation. (Source: Ishiguri *et al.* 2010)